4

Electromagnetic Formalisms for Optical Propagation in Three-Dimensional Periodic Liquid-Crystal Microstructures

I-Lin Ho and Yia-Chung Chang
Research Center for Applied Sciences, Academia Sinica, Taipei, Taiwan 115, R.O.C. Taiwan

1. Introduction

Nanoscale structures have achieved novel functions in liquid crystal devices such as liquid crystal displays, optical filters, optical modulators, phase conjugated systems, optical attenuators, beam amplifiers, tunable lasers, holographic data storage and even as parts for optical logic systems over the last decades (Blinov et al. (2006; 2007); Sutkowski et al. (2006)). Many theoretical works also have been reported on liquid crystal (LC) optics. Jones method (Jones (1941)) is first proposed for an easy calculation, which stratifies the media along the cell normal while remains the transverse LC orientation uniform, and hence supplies a straightforward way to analyze the forward propagation at normal incidence. This was later followed by the extended Jones method (Lien (1997)), which allows to trace the forward waves at an oblique incidence. The Berreman method (Berreman (1972)) then provides an alternative process to include forward and backward waves.

A further step in LC optics is to consider rigorously the LC variation both along the cell normal and along a single transverse direction, leading to a two-dimensional treatment of light propagation. This step is fulfilled by implementing the finite-difference time-domain method (Kriezis et al. (2000a); Witzigmann et al. (1998)), the vector beam propagation method (Kriezisa & Elston (1999); Kriezis & Elston (2000b)), coupled-wave theory (Galatola et al. (1994); Rokushima & Yamakita (1983)), and an extension of the Berreman approach (Zhang & Sheng (2003)), and has proven to be successful in demonstrating the strong scattering and diffractive effects on the structures with transverse LC variation lasting over the optical-wavelength scale.

For three-dimensional LC medium with arbitrary normal and transverse LC variations, Kriezis et al. (2002) proposed a composite scheme based on the finite-difference time-domain method and the plane-wave expansion method to evaluate the light propagation in periodic liquid-crystal microstructures. Olivero & Oldano (2003) applied numerical calculations by a standard spectral method and the finite-difference frequency-domain method for electromagnetic propagation in LC cells. Glytsis & Gaylord (1987) gave three-dimensional coupled-wave diffraction algorithms via the field decomposition into ordinary and extraordinary waves, although the transverse variation of the ordinary/extraordinary axis raises the complexity. Alternatively, this work neglects the multiple reflections and gives a coupling-matrix algorithm that is much easier to manipulate algebraically for three-dimensional LC media, yet accounts for the effects of the Fresnel refraction and

the single reflection at the surfaces of the media. The detailed derivations are described in appendix A. Furthermore, analogous with the Berreman approach (Berreman (1972)) to consider the multiple reflections for one-dimensional layered media (i.e. stratifying the media along the cell normal while remaining the transverse LC orientation uniform), another supplementary formulae including the influences of multiple reflections for three-dimensional media (i.e. stratifying the media along the cell normal and simultaneously including the varying LC orientation along the transverse) are also addressed in the appendix A. The program code of wolfram mathematica for coupling-matrix method is appended in appendix B for references.

2. Extended Jones matrix method revisited

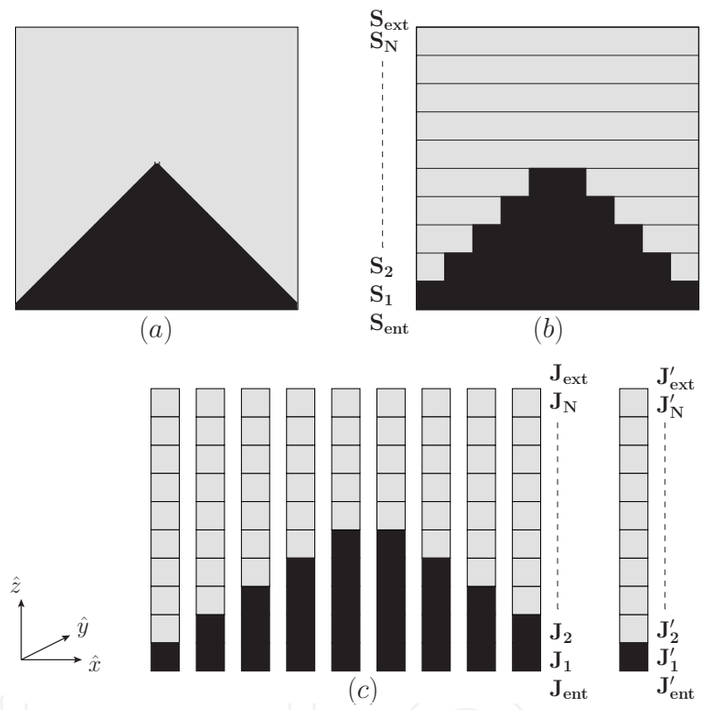

Fig. 1. (a) Schematic depiction of one unit cell of the periodic LC structures. (b) Stratification of the cell along the cell normal $\hat{z}$ with remaining the real transverse $\hat{x}(\hat{y})$ profile as in coupling-matrix method.(c) Decompose the cell along the transverse direction $\hat{x}(\hat{y})$ into independent strips, and treat the stratification of each stripe with uniform transverse profiles, as in (extended) Jones matrix method.

In this section, extended Jones matrix method is revisited first due to its similar underlying concepts can supply an accessibility to understand the coupling-matrix method. In the extended Jones matrix method, the liquid crystal cell (Figure 1(a)) is decomposed into multiple one-dimensional (z) independent stripes (Figure 1(c)), treating the transverse LC orientation uniform within each stripes and being irrelevant each other. Each stripe is further divided into N layers along the z direction, including two separate polarizer and analyzer layers. In the layer, there are four eigen-mode waves: two transmitted and two reflected waves; while at the interface of the layer, the boundary condition is that the tangential components of the electric field are continuous. Without loss of generality, considering the propagation of waves

in the xz plane at angle angle θ related to z axis, it specifies $\vec{k} = (k_0 sin\theta, 0, k_0 cos\theta)$, extended Jones Matrix can relate the electric fields at the bottom of the ℓ_{th} layer to the fields at the top of the ℓ_{th} layer of each strip by:

$$\begin{bmatrix} E_x \\ E_y \end{bmatrix}_{\ell, dz_\ell} = \mathbf{J}_\ell \begin{bmatrix} E_x \\ E_y \end{bmatrix}_{\ell,0} ; \ \mathbf{J}_\ell = \mathbf{A}_\ell \mathbf{\Xi}_\ell \mathbf{A}_\ell^{-1} \tag{1}$$

with

$$\mathbf{\Xi}_\ell = \begin{bmatrix} \exp(ik_{z1} dz_\ell) & 0 \\ 0 & \exp(ik_{z2} dz_\ell) \end{bmatrix}; \quad \mathbf{A}_\ell = \begin{bmatrix} e_{x1} & e_{x2} \\ e_{y1} & e_{y2} \end{bmatrix} \tag{2}$$

$$\frac{k_{z1}}{k_0} = \left(n_0^2 - \frac{k_x^2}{k_0^2} \right)^{1/2}; \tag{3}$$

$$\frac{k_{z2}}{k_0} = -\frac{\varepsilon_{xz}}{\varepsilon_{zz}} \frac{k_x}{k_0} + \frac{n_o n_e}{\varepsilon_{zz}} \left(\varepsilon_{zz} - \left(1 - \frac{n_e^2 - n_o^2}{n_e^2} \cos^2\theta_o \sin^2\phi_o \right) \frac{k_x^2}{k_0^2} \right)^{1/2} \tag{4}$$

$$e_{x1} = \left(\frac{k_{z1}^2}{k_0^2} + \frac{k_x^2}{k_0^2} - \varepsilon_{yy} \right) \left(\frac{k_x^2}{k_0^2} - \varepsilon_{zz} \right) - \varepsilon_{yz}\varepsilon_{zy} \tag{5}$$

$$e_{y1} = \left(\frac{k_x^2}{k_0^2} - \varepsilon_{zz} \right) \varepsilon_{yx} + \left(\frac{k_x}{k_0} \frac{k_{z1}}{k_0} + \varepsilon_{zx} \right) \varepsilon_{yz} \tag{6}$$

$$e_{x2} = \left(-\frac{k_x^2}{k_0^2} + \varepsilon_{zz} \right) \varepsilon_{xy} - \left(\frac{k_x}{k_0} \frac{k_{z2}}{k_0} + \varepsilon_{xz} \right) \varepsilon_{zy} \tag{7}$$

$$e_{y2} = \left(-\frac{k_{z2}^2}{k_0^2} + \varepsilon_{xx} \right) \left(\frac{k_x^2}{k_0^2} - \varepsilon_{zz} \right) + \left(\frac{k_x}{k_0} \frac{k_{z2}}{k_0} + \varepsilon_{zx} \right) \left(\frac{k_x}{k_0} \frac{k_{z2}}{k_0} + \varepsilon_{xz} \right) \tag{8}$$

Here, $k_0 = \omega/c = 2\pi/\lambda$ with λ the wavelength of the incident light in free space. dz_ℓ is the thickness of the the ℓ_{th} layer. θ_o and ϕ_o are the orientation angles of the LC director defined in the spherical coordinate. $\varepsilon_{i,j\in\{x,y,z\}}$ is the dielectric tensors defined in appendix A. Equation (1) can be understood as follow. $\mathbf{A}_\ell^{-1}$ transforms the electric fields at the bottom of the ℓ_{th} layer into the eigen-mode fields. $\mathbf{\Xi}_\ell$ then propagates the eigen-mode fields from the bottom of the ℓ_{th} layer to the top of the ℓ_{th} layer through the distance dz_ℓ. Finally, $\mathbf{A}_\ell$ transform the eigen-mode fields at the top of the the ℓ_{th} layer back into the electric fields at the top of the ℓ_{th} layer, which is equal to the electric fields at the bottom of the $(\ell+1)_{th}$ layer by boundary condition. Grouping all layers, the extended Jones matrix formula that relates the incident electric fields ($\ell = 0$) and the emitted electric fields ($\ell = N+1$) is given by

$$\begin{bmatrix} E_x \\ E_y \end{bmatrix}_{N+1} = \mathbf{J}_{ext} \mathbf{J}_N \mathbf{J}_{N-1} \cdots \mathbf{J}_2 \mathbf{J}_1 \mathbf{J}_{ent} \begin{bmatrix} E_x \\ E_y \end{bmatrix}_0 \tag{9}$$

$$\mathbf{J}_{ent} = \begin{bmatrix} \frac{2\cos\theta_p}{\cos\theta_p + n_p \cos\theta} & 0 \\ 0 & \frac{2\cos\theta}{\cos\theta + n_p \cos\theta_p} \end{bmatrix} \tag{10}$$

$$\mathbf{J}_{ext} = \begin{bmatrix} \frac{2n_p\cos\theta}{\cos\theta_p + n_p \cos\theta} & 0 \\ 0 & \frac{2n_p\cos\theta_p}{\cos\theta + n_p \cos\theta_p} \end{bmatrix} \tag{11}$$

with $\theta_p = \sin^{-1}(\sin\theta/\Re(n_p))$ in which $\Re(n_p)$ stands for the average of the real parts of the two indices of refraction (n_e and n_o) of the polarizer. The total transmission for the stripe is calculated by

$$trans. = \frac{|E_{x,N+1}|^2 + \cos^2\theta \cdot |E_{y,N+1}|^2}{|E_{x,0}|^2 + \cos^2\theta \cdot |E_{y,0}|^2} \tag{12}$$

The total transmission of the three-dimensional LC media then can be evaluated by summing up the contributions from the individual stripe.

3. Coupling matrix method

Parallel to the equation (9) by one-dimensional treatments for strips, an analogous coupling-matrix formulae for the propagations of waves through the three-dimensional periodic microstructures can be given as:

$$\begin{bmatrix} \vec{E}^+_{q,N+1} \\ \vec{M}^+_{q,N+1} \\ \vec{E}^-_{q,N+1} \\ \vec{M}^-_{q,N+1} \end{bmatrix} = \mathbf{S}_{ext}\mathbf{S}_N ... \mathbf{S}_2\mathbf{S}_1\mathbf{S}_{ent} \begin{bmatrix} \vec{E}^+_{q,0} \\ \vec{M}^+_{q,0} \\ \vec{E}^-_{q,0} \\ \vec{M}^-_{q,0} \end{bmatrix} \tag{13}$$

Here, $\vec{E}^+_{q,\ell}$ and $\vec{M}^+_{q,\ell}$ ($\vec{E}^-_{q,\ell}$ and $\vec{M}^-_{q,\ell}$) represent the physical forward (backward) TE and TM fields, i.e. transverse electric and transverse magnetic fields corresponding to the planes of the diffraction waves in the incident ($\ell = 0$) and emitted ($\ell = N+1$) regions. In which the components of the vectors $\vec{E}^+_{q,\ell}$, $\vec{M}^+_{q,\ell}$, $\vec{E}^-_{q,\ell}$, or $\vec{M}^-_{q,\ell}$ define the diffraction waves along the direction $\mathbf{n}_{gh} = n_{xg}\hat{\imath} + n_{yh}\hat{\jmath} + \xi_{gh}\hat{k}$:

$$n_{xg} = n_I \sin\theta\cos\phi - g\frac{\lambda}{\Lambda_x} \tag{14}$$

$$n_{yh} = n_I \sin\theta\sin\phi - h\frac{\lambda}{\Lambda_y} \tag{15}$$

$$\xi_{gh} = \sqrt{\varepsilon_{I(E)} - n_{yh}n_{yh} - n_{xg}n_{xg}} \tag{16}$$

with $\varepsilon_I = n_I^2$ ($\varepsilon_E = n_E^2$) being the dielectric coefficient in the incident (emitted) region. Note that the components with imaginary ξ_{gh} values are ignored for studied cases due to the decaying natures along the electromagnetic propagations parallel to the z direction. Λ_x (Λ_y) is the periodicity of the LC structure along the x (y) direction. $\mathbf{S}_{\ell\in\{1\sim N\}}$ is the matrix representing the propagations of waves through the ℓ_{th} structured layer. It consists of the matrix $\mathbf{T}^{(a)}_\ell$, which is the (column) eigen-vector matrix of the characteristic matrix $\mathbf{G}_\ell$ for the ℓ_{th} layer , and the diagonal matrix $exp\left[i\kappa^{(a)}_\ell \overline{dz}_\ell\right]$ relates to the eigen-value $\kappa^{(a)}_\ell$ of $\mathbf{G}_\ell$ with dimensionless $\overline{dz}_\ell = dz_\ell k_0$:

$$\mathbf{S}_\ell = \mathbf{T}^{(a)}_\ell exp\left[i\kappa^{(a)}_\ell \overline{dz}_\ell\right](\mathbf{T}^{(a)}_\ell)^{-1} \tag{17}$$

$$\mathbf{G}_\ell = \begin{bmatrix} \tilde{n}_x\tilde{\varepsilon}_{zz}^{-1}\tilde{\varepsilon}_{zx} & \tilde{n}_x\tilde{\varepsilon}_{zz}^{-1}\tilde{n}_x - 1 & \tilde{n}_x\tilde{\varepsilon}_{zz}^{-1}\tilde{\varepsilon}_{zy} & -\tilde{n}_x\tilde{\varepsilon}_{zz}^{-1}\tilde{n}_y \\ \tilde{\varepsilon}_{xz}\tilde{\varepsilon}_{zz}^{-1}\tilde{\varepsilon}_{zx} - \tilde{\varepsilon}_{xx} + \tilde{n}_y\tilde{n}_y & \tilde{\varepsilon}_{xz}\tilde{\varepsilon}_{zz}^{-1}\tilde{n}_x & \tilde{\varepsilon}_{xz}\tilde{\varepsilon}_{zz}^{-1}\tilde{\varepsilon}_{zy} - \tilde{\varepsilon}_{xy} - \tilde{n}_y\tilde{n}_x & -\tilde{\varepsilon}_{xz}\tilde{\varepsilon}_{zz}^{-1}\tilde{n}_y \\ \tilde{n}_y\tilde{\varepsilon}_{zz}^{-1}\tilde{\varepsilon}_{zx} & \tilde{n}_y\tilde{\varepsilon}_{zz}^{-1}\tilde{n}_x & \tilde{n}_y\tilde{\varepsilon}_{zz}^{-1}\tilde{\varepsilon}_{zy} & -\tilde{n}_y\tilde{\varepsilon}_{zz}^{-1}\tilde{n}_y + 1 \\ -\tilde{\varepsilon}_{yz}\tilde{\varepsilon}_{zz}^{-1}\tilde{\varepsilon}_{zx} + \tilde{\varepsilon}_{yx} + \tilde{n}_x\tilde{n}_y & -\tilde{\varepsilon}_{yz}\tilde{\varepsilon}_{zz}^{-1}\tilde{n}_x & -\tilde{\varepsilon}_{yz}\tilde{\varepsilon}_{zz}^{-1}\tilde{\varepsilon}_{zy} + \tilde{\varepsilon}_{yy} - \tilde{n}_x\tilde{n}_x & \tilde{\varepsilon}_{yz}\tilde{\varepsilon}_{zz}^{-1}\tilde{n}_y \end{bmatrix} \tag{18}$$

In this context, the notation $\vec{E}$ (or $\vec{M}$) denotes the $N_gN_h \times 1$ vector with components E_{gh} (or M_{gh}) describing the wave along $\mathbf{n}_{gh}$. $\tilde{n}_x$ ($\tilde{n}_y$) are $N_gN_h \times N_gN_h$ diagonal matrices with N_gN_h diagonal elements n_{xg} (n_{yh}) being the same (g,h) sequence as that of $\vec{E}$ and $\vec{M}$, and are calculated by Equations (14-15). $\tilde{\varepsilon}_{ij\in\{x,y,z\}}$ are $N_gN_h \times N_gN_h$ matrices with elements $\varepsilon_{ij,\alpha\beta}$ being the Fourier transform of the spatial dielectric coefficients $\varepsilon_{ij}(x,y;z)$, in which the indexes α,β are arranged by the relation $\vec{M} \sim \tilde{\varepsilon}_{ij}\vec{E}$, i.e. $M_{gh} \sim \sum_{g'h'} \varepsilon_{ij,(g-g')(h-h')}E_{g'h'}$ (derived in appendix A). Above $N_{g(h)}$ define the number of considered total Fourier orders g (h) in the x (y) direction. 1 represents the $N_gN_h \times N_gN_h$ identity matrix. One may understand the Equation (17) for the ℓ_{th} layer by the similar way as described in extended Jones method: the $(\mathbf{T}_\ell^{(a)})^{-1}$ term represents the coordinate transformation from the spatial tangential components of fields $\mathbf{f}_{\hat{t},\ell} = [\vec{e}_{x,\ell}\ \vec{h}_{y,\ell}\ \vec{e}_{y,\ell}\ \vec{h}_{x,\ell}]^t$ denoted by Equations (46)-(47) at ℓ_{th} interface into the orthogonal components of the eigen-modes in the ℓ_{th} layer; the $exp\left[i\kappa_\ell^a\overline{dz}_\ell\right]$ term describes eigen-mode propagation over the distance $\overline{dz}_\ell$ (thickness of the ℓ_{th} layer); the $\mathbf{T}_\ell^{(a)}$ term then is the inversely coordinate transformation from the eigen-mode components back to the spatial tangential components of fields at the next interface. Considering the continuum of tangential fields on interfaces, these fields emitted from the ℓ_{th} layer hence can be straightforwardly treated as the incident fields $\mathbf{f}_{\hat{t},\ell+1}$ for the $(\ell+1)_{th}$ layer, and allow to follow the next transfer matrix $\mathbf{S}_{\ell+1}$ to describe the sequential propagations of fields through the $(\ell+1)_{th}$ layer as in Equation (13).

For the matrices $\mathbf{S}_{ent}$ and $\mathbf{S}_{ext}$ defined for the (isotropic) uniform incident ($\ell = 0$) and emitted ($\ell = N+1$) regions, respectively, the eigen-modes are specially chosen (and symbolized) as $\vec{E}_q^+$ and $\vec{M}_q^+$ ($\vec{E}_q^-$ and $\vec{M}_q^-$) (Ho et al. (2011); Rokushima & Yamakita (1983)), representing the physical forward (backward) TE and TM waves as the above-mentioned. In which the transform matrix $\mathbf{T}_{\varepsilon_I}^{(i)}$ between the eigen-mode components and the tangential components $\mathbf{f}_{\hat{t},0} = [\vec{e}_{x,0}\ \vec{h}_{y,0}\ \vec{e}_{y,0}\ \vec{h}_{x,0}]^t$ for the isotropic incident region ($\ell = 0$) is given as:

$$\begin{aligned} \begin{bmatrix} \vec{e}_{x,0} \\ \vec{h}_{y,0} \\ \vec{e}_{y,0} \\ \vec{h}_{x,0} \end{bmatrix} &= \begin{bmatrix} \dot{\mathbf{n}}_y & \dot{\mathbf{n}}_x & \dot{\mathbf{n}}_y & \dot{\mathbf{n}}_x \\ \dot{\mathbf{n}}_y\xi & \varepsilon_I\dot{\mathbf{n}}_x\xi^{-1} & -\dot{\mathbf{n}}_y\xi & -\varepsilon_I\dot{\mathbf{n}}_x\xi^{-1} \\ -\dot{\mathbf{n}}_x & \dot{\mathbf{n}}_y & -\dot{\mathbf{n}}_x & \dot{\mathbf{n}}_y \\ \dot{\mathbf{n}}_x\xi & -\varepsilon_I\dot{\mathbf{n}}_y\xi^{-1} & -\dot{\mathbf{n}}_x\xi & \varepsilon_I\dot{\mathbf{n}}_y\xi^{-1} \end{bmatrix} \begin{bmatrix} \vec{E}_{q,0}^+ \\ \vec{M}_{q,0}^+ \\ \vec{E}_{q,0}^- \\ \vec{M}_{q,0}^- \end{bmatrix} \\ &\equiv \mathbf{T}_{\varepsilon_I}^{(i)} \begin{bmatrix} \vec{E}_{q,0}^+ \\ \vec{M}_{q,0}^+ \\ \vec{E}_{q,0}^- \\ \vec{M}_{q,0}^- \end{bmatrix} \end{aligned} \tag{19}$$

Here, $\dot{\mathbf{n}}_y$ and $\dot{\mathbf{n}}_x$ are $N_gN_h \times N_gN_h$ diagonal matrices with normalized elements $\frac{n_{yh}}{m_{gh}}$ and $\frac{n_{xg}}{m_{gh}}$ respectively. ξ^{-1} is the diagonal matrix with elements $1/\xi_{gh}$ (not the inverse of the matrix ξ),

in which $m_{gh} = (n_{yh}n_{yh} + n_{xg}n_{xg})^{1/2}$, $\xi_{gh} = (\varepsilon_I - n_{yh}n_{yh} - n_{xg}n_{xg})^{1/2}$, and $\varepsilon_I = n_I^2$ have been applied for the incident region. A similar transform for $\mathbf{f}_{\hat{t},N+1}$ in the emitted region can be derived straightforwardly by replacing all the ε_I in Equation (19) with ε_E and can be denoted as $\mathbf{f}_{\hat{t},N+1} = \mathbf{T}_{\varepsilon_E}^{(i)}[\vec{E}_{q,N+1}^{+}\ \vec{M}_{q,N+1}^{+}\ \vec{E}_{q,N+1}^{-}\ \vec{M}_{q,N+1}^{-}]^t$, with $\xi_{gh} = (\varepsilon_E - n_{yh}n_{yh} - n_{xg}n_{xg})^{1/2}$, and $\varepsilon_E = n_E^2$.

$\mathbf{S}_{ent}$ is the matrix representing the light propagation from the incident region into the medium, and indicates the essential refraction and the reflection at the first interface of the medium. To consider these effects in a simple way, a virtual (isotropic) uniform layer, which has zero thickness and effective dielectric coefficient $\varepsilon_a = n_{avg}^2$, e.g. $n_{avg} = (n_e + n_o)/2$ for the liquid-crystal grating, is assumed to exist between the incident region and the 1_{st} layer. $\mathbf{S}_{ent}$ thereby can be approximately evaluated as:

$$\mathbf{S}_{ent} = \mathbf{T}_{\varepsilon_a}^{(i)} \begin{bmatrix} \mathbf{W}_1'^{-1} & \mathbf{0} \\ \mathbf{0} & \mathbf{0} \end{bmatrix} \tag{20}$$

$$\begin{bmatrix} \mathbf{W}_1' & \mathbf{W}_2' \\ \mathbf{W}_3' & \mathbf{W}_4' \end{bmatrix} = \left[(\mathbf{T}_{\varepsilon_a}^{(i)})^{-1} \mathbf{T}_{\varepsilon_I}^{(i)} \right]^{-1} \tag{21}$$

Here, $\mathbf{T}_{\varepsilon_a}^{(i)}$ is formulated as equation (19) with the replacements of ε_I by ε_a, $\xi_{gh} = (\varepsilon_a - n_{yh}n_{yh} - n_{xg}n_{xg})^{1/2}$, and $\varepsilon_a = n_{avg}^2$. Similar to the argument of $\mathbf{S}_{ent}$, another virtual (isotropic) uniform layer is included between the emitted region and the N_{th} layer to consider the effects of refraction and the reflection at the last interface. Here, $\mathbf{S}_{ext}$ is approximated as:

$$\mathbf{S}_{ext} = \begin{bmatrix} \mathbf{W}_1''^{-1} & \mathbf{0} \\ \mathbf{0} & \mathbf{0} \end{bmatrix} (\mathbf{T}_{\varepsilon_a}^{(i)})^{-1} \tag{22}$$

$$\begin{bmatrix} \mathbf{W}_1'' & \mathbf{W}_2'' \\ \mathbf{W}_3'' & \mathbf{W}_4'' \end{bmatrix} = \left[(\mathbf{T}_{\varepsilon_E}^{(i)})^{-1} \mathbf{T}_{\varepsilon_a}^{(i)} \right]^{-1} \tag{23}$$

Put everything together, and the propagation of fields through three-dimensional periodic microstructures hence can be evaluated as in Equation (13).

4. Numerical analyses

In this section, a simple case is applied to demonstrate the algorithms and is verified by finite-difference time-domain (FDTD) method. Consider a one-layer film ($N = 1$) with liquid-crystal orientation $\theta_o = \pi x/\Lambda_x = \lambda\overline{x}/2\Lambda_x$, $\phi_o = \pi/2$. By the Fourier transform defined in equations (42-45), the non-zero Fourier components for the dielectric elements $\overline{\varepsilon}_{ij,gh}$ are: $\overline{\varepsilon}_{xx,00} = n_o^2$, $\overline{\varepsilon}_{yy,00} = \left(n_o^2 + n_e^2\right)/2$, $\overline{\varepsilon}_{yy,\pm 10} = \left(n_o^2 - n_e^2\right)/4$, $\overline{\varepsilon}_{yz,\pm 10} = \pm i\left(n_o^2 - n_e^2\right)/4$, $\overline{\varepsilon}_{zz,00} = \left(n_o^2 + n_e^2\right)/2$, $\overline{\varepsilon}_{zz,\pm 10} = \left(n_e^2 - n_o^2\right)/4$. For simplicity, we only consider three Fourier components of fields, i.e. $(g,h) = (\pm 1, 0)$ and $(0,0)$, for this case. The corresponding transfer-matrix formula in equation (13) are then given as:

$$\begin{bmatrix} \vec{E}_{q,N+1}^{+} \\ \vec{M}_{q,N+1}^{+} \\ \vec{E}_{q,N+1}^{-} \\ \vec{M}_{q,N+1}^{-} \end{bmatrix} = \mathbf{S}_{ext}\mathbf{S}_1\mathbf{S}_{ent} \begin{bmatrix} \vec{E}_{q,0}^{+} \\ \vec{M}_{q,0}^{+} \\ \vec{E}_{q,0}^{-} \\ \vec{M}_{q,0}^{-} \end{bmatrix} \tag{24}$$

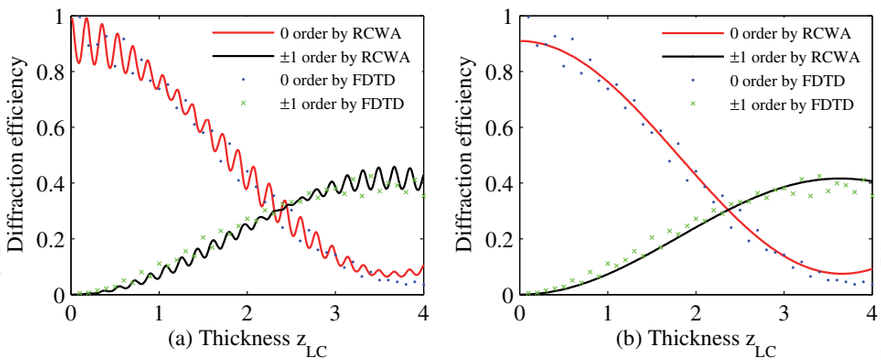

Fig. 2. Diffraction efficiency for the periodic LC structures at thickness $z_{LC} = 0 - 4\mu m$, in which (a) the solid line indicates numerical results by RCWA with considering multiple reflections as in the appendix (equations 89-92), and are in agreement with those (dotted line) from the FDTD method, while (b) the solid line indicates numerical results by the RCWA with ignoring multiple reflections, yet accounting for the effects of the Fresnel refraction and the single reflection at the surfaces of the media as in equation (13), showing comparable results.

which relates to the eigen-vector matrices $\mathbf{T}_0/\mathbf{T}_2$ for the isotropic incident/emitted layer in the equation (19), and the eigen-values $\kappa_1^{(a)}$ and eigen-vector $\mathbf{T}_1^{(a)}$ matrices of $\mathbf{G}$ in equation (18) for the liquid-crystal film. Here, $z_{lc} = \overline{z}_{lc}/k_0$ is the thickness of the liquid-crystal film. In this case, we simply choose the unit-amplitude normal TE incidence with respect to the xz incident plane, i.e. $\vec{E}_{q,0}^{+} = \left[E_{q,0,-10}^{+} \; E_{q,0,00}^{+} \; E_{q,0,10}^{+} \right]^t = \left[0 \; 1 \; 0 \right]^t$ and $\vec{M}_{q,0}^{+} = \left[M_{q,0,-10}^{+} \; M_{q,0,00}^{+} \; M_{q,0,10}^{+} \right]^t = \left[0 \; 0 \; 0 \right]^t$. For the isotropic incident/emitted air layer ($\varepsilon = 1$), the associated $\dot{\mathbf{n}}_x$, $\dot{\mathbf{n}}_y$, ε, and ξ in $\mathbf{T}_0/\mathbf{T}_2$ are referred to equations (14,15,16), and are given as:

$$\dot{\mathbf{n}}_x = \begin{bmatrix} 1 & 0 & 0 \\ 0 & 1 & 0 \\ 0 & 0 & -1 \end{bmatrix}; \dot{\mathbf{n}}_y = \begin{bmatrix} 0 & 0 & 0 \\ 0 & 0 & 0 \\ 0 & 0 & 0 \end{bmatrix}; \varepsilon = \begin{bmatrix} 1 & 0 & 0 \\ 0 & 1 & 0 \\ 0 & 0 & 1 \end{bmatrix} \tag{25}$$

$$\xi = \begin{bmatrix} \sqrt{1 - \lambda^2/\Lambda_x^2} & 0 & 0 \\ 0 & 1 & 0 \\ 0 & 0 & \sqrt{1 - \lambda^2/\Lambda_x^2} \end{bmatrix} \tag{26}$$

$$\xi^{-1} = \begin{bmatrix} 1/\sqrt{1 - \lambda^2/\Lambda_x^2} & 0 & 0 \\ 0 & 1 & 0 \\ 0 & 0 & 1/\sqrt{1 - \lambda^2/\Lambda_x^2} \end{bmatrix} \tag{27}$$

Note we have used a small incident angle ($\theta = 10^{-5}$, $\phi = 0$) to avoid the numerical instability at $\theta = 0$. For the layer of liquid-crystal film, the associated $\tilde{\mathbf{n}}_x$, $\tilde{\mathbf{n}}_y$ and $\varepsilon_{ij\in\{x,y,z\}}$ in $\mathbf{G}$ in equation (18) are written out as below:

$$\tilde{\mathbf{n}}_x = \begin{bmatrix} \lambda/\Lambda_x & 0 & 0 \\ 0 & 1 & 0 \\ 0 & 0 & -\lambda/\Lambda_x \end{bmatrix}; \tilde{\mathbf{n}}_y = \begin{bmatrix} 0 & 0 & 0 \\ 0 & 0 & 0 \\ 0 & 0 & 0 \end{bmatrix} \tag{28}$$

$$\varepsilon_{xx} = \begin{bmatrix} \varepsilon_{xx,00} & \varepsilon_{xx,-10} & \varepsilon_{xx,-20} \\ \varepsilon_{xx,10} & \varepsilon_{xx,00} & \varepsilon_{xx,-10} \\ \varepsilon_{xx,20} & \varepsilon_{xx,10} & \varepsilon_{xx,00} \end{bmatrix} = \begin{bmatrix} n_o^2 & 0 & 0 \\ 0 & n_o^2 & 0 \\ 0 & 0 & n_o^2 \end{bmatrix} \tag{29}$$

$$\varepsilon_{yy} = \begin{bmatrix} \frac{n_o^2+n_e^2}{2} & \frac{n_o^2-n_e^2}{4} & 0 \\ \frac{n_o^2-n_e^2}{4} & \frac{n_o^2+n_e^2}{2} & \frac{n_o^2-n_e^2}{4} \\ 0 & \frac{n_o^2-n_e^2}{4} & \frac{n_o^2+n_e^2}{2} \end{bmatrix} \tag{30}$$

$$\varepsilon_{zz} = \begin{bmatrix} \frac{n_o^2+n_e^2}{2} & \frac{n_e^2-n_o^2}{4} & 0 \\ \frac{n_e^2-n_o^2}{4} & \frac{n_o^2+n_e^2}{2} & \frac{n_e^2-n_o^2}{4} \\ 0 & \frac{n_e^2-n_o^2}{4} & \frac{n_o^2+n_e^2}{2} \end{bmatrix} \tag{31}$$

$$\varepsilon_{yz} = \begin{bmatrix} 0 & \frac{-i\left(n_o^2-n_e^2\right)}{4} & 0 \\ \frac{i\left(n_o^2-n_e^2\right)}{4} & 0 & \frac{-i\left(n_o^2-n_e^2\right)}{4} \\ 0 & \frac{i\left(n_o^2-n_e^2\right)}{4} & 0 \end{bmatrix} \tag{32}$$

$$\varepsilon_{xy} = 0, \quad \varepsilon_{xz} = 0 \tag{33}$$

Consequently, the eigen-values $\kappa_1^{(a)}$ and eigen-vector $\mathbf{T}_1^{(a)}$ matrices of $\mathbf{G}$ can be numerically evaluated and a similar process for $\mathbf{S}_{ent}$ and $\mathbf{S}_{ext}$ can be followed straightforwardly. Together with all these definitions of matrixes in equation (24), the transmittance fields $\vec{E}_{q,2}^{+}$ and $\vec{M}_{q,2}^{+}$ then can be decided. Here, we set $\lambda = 0.55um$, $\Lambda_x = 2.0um$, $n_o = 1.5$, and $n_e = 1.6$. The numerical results of far-field diffractions for this case by RCWA ignoring the influences of the multiple reflections are shown in figure 2(b), and are in agreement with these obtained by FDTD. Besides, an alternative consideration described by the equations (89-92) in appendix A, which includes the multiple reflections, is shown in figure 2(a), and clarifies the effectiveness of the easy-manipulated algorithm in equation (13) for the three-dimensional periodic LC media.

A. Derivation of the coupling matrix

In this appendix, detailed derivations of the coupling matrix method are demonstrated for references.

A.1 Maxwell's equations in spatial-space descriptions

Without charges and currents, Maxwell's equations can be read as:

$$\nabla \cdot \mathbf{E} = 0 \tag{34}$$

$$\nabla \cdot \mathbf{B} = 0 \tag{35}$$

$$\nabla \times \mathbf{E} = -\frac{\partial \mathbf{B}}{\partial t} \tag{36}$$

$$\nabla \times \mathbf{B} = \mu\mu_0\varepsilon\varepsilon_0 \frac{\partial \mathbf{E}}{\partial t} \tag{37}$$

Define variables $k_0 = \omega\sqrt{\mu_0\varepsilon_0} = \frac{2\pi}{\lambda}$, $Y_0 = \frac{1}{Z_0} = \sqrt{\frac{\varepsilon_0}{\mu_0}}$, $\overline{r} = k_0 r$, $\overline{x} = k_0 x$, $\overline{y} = k_0 y$, $\overline{z} = k_0 z$, and $\overline{\nabla}_i = \partial/\partial\overline{r}_i = \partial/\partial r_i k_0 = \nabla_i/k_0$, and the equations can be derived as:

$$\overline{\nabla}\cdot\mathbf{E} = 0 \tag{38}$$

$$\overline{\nabla}\cdot\mathbf{B} = 0 \tag{39}$$

$$\overline{\nabla}\times\sqrt{Y_0}\mathbf{E} = -i\sqrt{Z_0}\mathbf{H} \tag{40}$$

$$\begin{aligned}\overline{\nabla}\times\sqrt{Z_0}\mathbf{H} &= i\overline{\varepsilon}\left(\overline{r}\right)\sqrt{Y_0}\mathbf{E}\\ &= i\begin{bmatrix}\overline{\varepsilon}_{xx}\left(\overline{r}\right) & \overline{\varepsilon}_{xy}\left(\overline{r}\right) & \overline{\varepsilon}_{xz}\left(\overline{r}\right)\\ \overline{\varepsilon}_{yx}\left(\overline{r}\right) & \overline{\varepsilon}_{yy}\left(\overline{r}\right) & \overline{\varepsilon}_{yz}\left(\overline{r}\right)\\ \overline{\varepsilon}_{zx}\left(\overline{r}\right) & \overline{\varepsilon}_{zy}\left(\overline{r}\right) & \overline{\varepsilon}_{zz}\left(\overline{r}\right)\end{bmatrix}\sqrt{Y_0}\mathbf{E}\end{aligned} \tag{41}$$

Here, all the field components are assumed to have time dependence of $\exp(i\omega t)$ and are omitted everywhere. The relative permeability of the medium is assumed to be $\mu = 1$. Note that $\varepsilon_{ij\in\{x,y,z\}}$ are defined as functions of position (x, y, z) and $\overline{\varepsilon}_{ij}$ are of $(\overline{x}, \overline{y}, \overline{z})$. λ is the vacuum wavelength of the incident wave. Variables x, y, z generally represent spatial positions while these appeared in suffix, e.g $\varepsilon_{ij\in\{x,y,z\}}$, denote the orientations along the directions $\hat{x}, \hat{y}, \hat{z}$. Moreover, the variable i is the imaginary constant number $i = \sqrt{-1}$ and that appeared in suffix, e.g. dz_i, is an integer indexing number. For liquid crystals, the dielectric matrix ε is associated with the orientation of director (θ_o, ϕ_o):

$$\varepsilon = \begin{bmatrix}\varepsilon_{xx} & \varepsilon_{xy} & \varepsilon_{xz}\\ \varepsilon_{yx} & \varepsilon_{yy} & \varepsilon_{yz}\\ \varepsilon_{zx} & \varepsilon_{zy} & \varepsilon_{zz}\end{bmatrix} \tag{42}$$

with

$$\begin{aligned}\varepsilon_{xx} &= n_o^2 + \left(n_e^2 - n_o^2\right)\sin^2\theta_o\cos^2\phi_o,\\ \varepsilon_{xy} &= \varepsilon_{yx} = \left(n_e^2 - n_o^2\right)\sin^2\theta_o\sin\phi_o\cos\phi_o,\\ \varepsilon_{xz} &= \varepsilon_{zx} = \left(n_e^2 - n_o^2\right)\sin\theta_o\cos\theta_o\cos\phi_o,\\ \varepsilon_{yy} &= n_o^2 + \left(n_e^2 - n_o^2\right)\sin^2\theta_o\sin^2\phi_o,\\ \varepsilon_{yz} &= \varepsilon_{zy} = \left(n_e^2 - n_o^2\right)\sin\theta_o\cos\theta_o\sin\phi_o,\\ \varepsilon_{zz} &= n_o^2 + \left(n_e^2 - n_o^2\right)\cos^2\theta_o,\end{aligned} \tag{43}$$

where n_e and n_o are extraordinary and ordinary indices of refraction of the birefringent liquid crystal, respectively, θ_o is the angle between the director and the z axis, and ϕ_o is the angle between the projection of the director on the xy plane and x axis.

A.2 Maxwell's equations in k-space descriptions

Consider the general geometry illustrated in Figure 3 of stacked multi-layer two-dimensional periodic microstructures. To apply the rigorous coupled-wave theory to the stack, all of the layers have to define the same periodicity: Λ_x along the x direction and Λ_y along the y

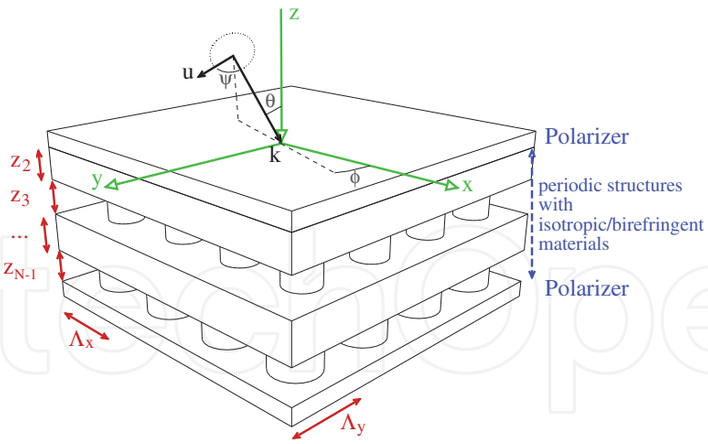

Fig. 3. Geometry of three-dimensional RCWA algorithm for a multi-layer stack with two-dimensional periodic microstructures in arbitrary isotropic and birefringent material arrangement.

direction. The thickness for the ℓ_{th} layer is dz_ℓ, and these layers contribute to a total thickness of the stack $Z_N = \sum_{\ell=1}^{N} dz_\ell$. The periodic permittivity of an individual layer in the stack can be expanded in Fourier series of the spatial harmonics as:

$$\overline{\varepsilon}_{ij}\left(\overline{x},\overline{y};\overline{z}_\ell\right) = \sum_{g,h} \overline{\varepsilon}_{ij,gh}\left(\overline{z}_\ell\right) \exp\left(i\frac{g\lambda\overline{x}}{\Lambda_x} + i\frac{h\lambda\overline{y}}{\Lambda_y}\right) \tag{44}$$

$$\overline{\varepsilon}_{ij,gh}\left(\overline{z}_\ell\right) = \frac{\lambda}{2\pi\Lambda_x}\frac{\lambda}{2\pi\Lambda_y}\int_0^{\frac{2\pi\Lambda_x}{\lambda}}\int_0^{\frac{2\pi\Lambda_y}{\lambda}} \overline{\varepsilon}_{ij}\left(\overline{x},\overline{y};\overline{z}_\ell\right) \exp\left(-i\frac{g\lambda\overline{x}}{\Lambda_x} - i\frac{h\lambda\overline{y}}{\Lambda_y}\right) d\overline{x}d\overline{y} \tag{45}$$

A similar transform for the fields in the stack can be expressed in terms of Rayleigh expansions:

$$\sqrt{Y_0}\mathbf{E}\left(\overline{x},\overline{y};\overline{z}_\ell\right) = \sum_{g,h} \mathbf{e}_{gh}\left(\overline{z}_\ell\right) \exp\left[-i\left(n_{xg}\overline{x} + n_{yh}\overline{y}\right)\right] \tag{46}$$

$$\sqrt{Z_0}\mathbf{H}\left(\overline{x},\overline{y};\overline{z}_\ell\right) = \sum_{g,h} \mathbf{h}_{gh}\left(\overline{z}_\ell\right) \exp\left[-i\left(n_{xg}\overline{x} + n_{yh}\overline{y}\right)\right] \tag{47}$$

$$n_{xg} = n_I \sin\theta\cos\phi - g\frac{\lambda}{\Lambda_x} \tag{48}$$

$$n_{yh} = n_I \sin\theta\sin\phi - h\frac{\lambda}{\Lambda_y} \tag{49}$$

where n_I (n_E) is the refraction index for the isotropic incident (emitted) region. θ, ϕ are the incident angles defined in sphere coordinates, and z is the normal direction for the xy plane of periodic structures. Here, the electric field of an incident unit-amplitude wave has been introduced by $\mathbf{E}_{inc} = \mathbf{u} \times exp\left(-i\mathbf{k}\cdot\mathbf{r}\right)$ as illustrated in figure 3, in which the wave vector $\mathbf{k}$ as well as the unit polarization vector $\mathbf{u}$ are given by:

$$\mathbf{k} = k_0 n_I \left(\sin\theta\cos\phi\hat{x} + \sin\theta\sin\phi\hat{y} + \cos\theta\hat{z}\right) \tag{50}$$

$$\begin{aligned}\mathbf{u} = u_x\hat{x} + u_y\hat{y} + u_z\hat{z} &= \left(\cos\Psi\cos\theta\cos\phi - \sin\Psi\sin\phi\right)\hat{x} \\ &+ \left(\cos\Psi\cos\theta\sin\phi + \sin\Psi\cos\phi\right)\hat{y} - \left(\cos\Psi\sin\theta\right)\hat{z}\end{aligned} \tag{51}$$

with the Ψ angle between the electric field vector and the incident plane.
Now we can express Maxwell's equations by the (g,h) Fourier components in k-space descriptions. For simplicity, we introduce the definitions of the tangential and normal fields at the interfaces as

$$\mathbf{f}_{\hat{t}} = \begin{bmatrix} \vec{e}_x \\ \vec{h}_y \\ \vec{e}_y \\ \vec{h}_x \end{bmatrix}, \quad \mathbf{f}_{\hat{n}} = \begin{bmatrix} \vec{e}_z \\ \vec{h}_z \end{bmatrix} \tag{52}$$

Here, $\vec{e}_{i\in\{x,y,z\}} = \vec{e}_i\left(\overline{z}_\ell\right)$ and $\vec{h}_{i\in\{x,y,z\}} = \vec{h}_i\left(\overline{z}_\ell\right)$ are column matrices with Fourier components $e_{i,gh}\left(\overline{z}_\ell\right)$ and $h_{i,gh}\left(\overline{z}_\ell\right)$, respectively. In the following context, a straightforward calculation to obtain the infinite set of coupled-wave equations corresponding to the infinite Fourier components is fulfilled. First, we express Maxwell's curl equations (40)-(41) in terms of the spatial x, y, z components:

$$\begin{aligned} \overline{\nabla} \times \sqrt{Y_0}\mathbf{E} &= \left[\partial_{\overline{x}}\sqrt{Y_0}E_y - \partial_{\overline{y}}\sqrt{Y_0}E_x\right]\hat{\mathbf{z}} + \left[\partial_{\overline{y}}\sqrt{Y_0}E_z - \partial_{\overline{z}}\sqrt{Y_0}E_y\right]\hat{\mathbf{x}} \\ &\quad + \left[\partial_{\overline{z}}\sqrt{Y_0}E_x - \partial_{\overline{x}}\sqrt{Y_0}E_z\right]\hat{\mathbf{y}} \\ &= -i\sqrt{Z_0}H_z\hat{\mathbf{z}} - i\sqrt{Z_0}H_x\hat{\mathbf{x}} - i\sqrt{Z_0}H_y\hat{\mathbf{y}} \end{aligned} \tag{53}$$

$$\begin{aligned} \overline{\nabla} \times \sqrt{Z_0}\mathbf{H} &= \left[\partial_{\overline{x}}\sqrt{Z_0}H_y - \partial_{\overline{y}}\sqrt{Z_0}H_x\right]\hat{\mathbf{z}} + \left[\partial_{\overline{y}}\sqrt{Z_0}H_z - \partial_{\overline{z}}\sqrt{Z_0}H_y\right]\hat{\mathbf{x}} \\ &\quad + \left[\partial_{\overline{z}}\sqrt{Z_0}H_x - \partial_{\overline{x}}\sqrt{Z_0}H_z\right]\hat{\mathbf{y}} \\ &= i\sqrt{Y_0}\left[\overline{\varepsilon}\left(\overline{r}\right)\mathbf{E}\right]_z\hat{\mathbf{z}} + i\sqrt{Y_0}\left[\overline{\varepsilon}\left(\overline{r}\right)\mathbf{E}\right]_x\hat{\mathbf{x}} + i\sqrt{Y_0}\left[\overline{\varepsilon}\left(\overline{r}\right)\mathbf{E}\right]_y\hat{\mathbf{y}} \end{aligned} \tag{54}$$

Next, we introduce the Fourier representations of $\mathbf{E}$, $\mathbf{H}$, and $\overline{\varepsilon}\left(\overline{r}\right)$ as defined in Equations (44)-(47). Maxwell's curl equations (53)-(54) can thereby be regrouped by the components of $\mathbf{f}_{\hat{t}}$ and $\mathbf{f}_{\hat{n}}$. For the component $h_{z,gh}\left(\overline{z}_\ell\right)$, the equation can be derived as:

$$\begin{aligned} \partial_{\overline{x}}\sqrt{Y_0}E_y - \partial_{\overline{y}}\sqrt{Y_0}E_x &= \sum_{gh} -in_{xg}e_{y,gh}\left(\overline{z}_\ell\right)\exp\left[-i\left(n_{xg}\overline{x} + n_{yh}\overline{y}\right)\right] \\ &\quad - \sum_{gh} -in_{yh}e_{x,gh}\left(\overline{z}_\ell\right)\exp\left[-i\left(n_{xg}\overline{x} + n_{yh}\overline{y}\right)\right] \\ &= -i\sqrt{Z_0}H_z = -i\sum_{gh} h_{z,gh}\left(\overline{z}_\ell\right)\exp\left[-i\left(n_{xg}\overline{x} + n_{yh}\overline{y}\right)\right] \end{aligned} \tag{55}$$

It is simplified to be:

$$h_{z,gh}\left(\overline{z}_\ell\right) = n_{xg}e_{y,gh}\left(\overline{z}_\ell\right) - n_{yh}e_{x,gh}\left(\overline{z}_\ell\right) \tag{56}$$

For the component $\frac{\partial e_{y,gh}\left(\overline{z}_\ell\right)}{\partial_{\overline{z}}}$, the equation can be derived as:

$$\begin{aligned} \partial_{\overline{y}}\sqrt{Y_0}E_z - \partial_{\overline{z}}\sqrt{Y_0}E_y &= \sum_{gh} -in_{yh}e_{z,gh}\left(\overline{z}_\ell\right)\exp\left[-i\left(n_{xg}\overline{x} + n_{yh}\overline{y}\right)\right] \\ &\quad - \sum_{gh} \frac{\partial e_{y,gh}\left(\overline{z}_\ell\right)}{\partial_{\overline{z}}}\exp\left[-i\left(n_{xg}\overline{x} + n_{yh}\overline{y}\right)\right] \\ &= -i\sqrt{Z_0}H_x = -i\sum_{gh} h_{x,gh}\left(\overline{z}_\ell\right)\exp\left[-i\left(n_{xg}\overline{x} + n_{yh}\overline{y}\right)\right] \end{aligned} \tag{57}$$

and is simplified to be:

$$\frac{\partial e_{y,gh}\left(\overline{z}_{\ell}\right)}{\partial_{\overline{z}}} = -in_{yh}e_{z,gh}\left(\overline{z}_{\ell}\right) + ih_{x,gh}\left(\overline{z}_{\ell}\right) \tag{58}$$

For the component $\frac{\partial e_{x,gh}(\overline{z}_{\ell})}{\partial_{\overline{z}}}$, the equation can be derived as:

$$\begin{aligned}\partial_{\overline{z}}\sqrt{Y_0}E_x - \partial_{\overline{x}}\sqrt{Y_0}E_z &= \sum_{m}\frac{\partial e_{x,gh}\left(\overline{z}_{\ell}\right)}{\partial_{\overline{z}}}\exp\left[-i\left(n_{xg}\overline{x}+n_{yh}\overline{y}\right)\right] \\ &\quad -\sum_{gh}-in_{xg}e_{z,gh}\left(\overline{z}_{\ell}\right)\exp\left[-i\left(n_{xg}\overline{x}+n_{yh}\overline{y}\right)\right] \\ &= -i\sqrt{Z_0}H_y \\ &= -i\sum_{gh}h_{y,gh}\left(\overline{z}_{\ell}\right)\exp\left[-i\left(n_{xg}\overline{x}+n_{yh}\overline{y}\right)\right]\end{aligned} \tag{59}$$

and is simplified to be:

$$\frac{\partial e_{x,gh}\left(\overline{z}_{\ell}\right)}{\partial_{\overline{z}}} = -in_{xg}e_{z,gh}\left(\overline{z}_{\ell}\right) - ih_{y,gh}\left(\overline{z}_{\ell}\right) \tag{60}$$

For the component $e_{z,gh}$, the equation can be derived as:

$$\begin{aligned}\partial_{\overline{x}}\sqrt{Z_0}H_y - \partial_{\overline{y}}\sqrt{Z_0}H_x &= \sum_{gh}-in_{xg}h_{y,gh}\left(\overline{z}_{\ell}\right)\exp\left[-i\left(n_{xg}\overline{x}+n_{yh}\overline{y}\right)\right] \\ &\quad -\sum_{gh}-in_{yh}h_{x,gh}\left(\overline{z}_{\ell}\right)\exp\left[-i\left(n_{xg}\overline{x}+n_{yh}\overline{y}\right)\right] \\ &= i\sqrt{Y_0}\left[\overline{\varepsilon}\left(\overline{r}\right)\mathbf{E}\right]_z \\ &= i\sum_{ghuv}\overline{\varepsilon}_{zx,uv}e_{x,gh}\left(\overline{z}_{\ell}\right)\exp\left[-i\left(n_{x(g+u)}\overline{x}+n_{y(h+v)}\overline{y}\right)\right] \\ &\quad +i\sum_{ghuv}\overline{\varepsilon}_{zy,uv}e_{y,gh}\left(\overline{z}_{\ell}\right)\exp\left[-i\left(n_{x(g+u)}\overline{x}+n_{y(h+v)}\overline{y}\right)\right] \\ &\quad +i\sum_{ghuv}\overline{\varepsilon}_{zz,uv}e_{z,gh}\left(\overline{z}_{\ell}\right)\exp\left[-i\left(n_{x(g+u)}\overline{x}+n_{y(h+v)}\overline{y}\right)\right]\end{aligned} \tag{61}$$

and is simplified to be:

$$\begin{aligned}n_{yh}h_{x,gh}\left(\overline{z}_{\ell}\right) - n_{xg}h_{y,gh}\left(\overline{z}_{\ell}\right) &= \sum_{u'v'}\overline{\varepsilon}_{zx,(g-u')(h-v')}e_{x,u'v'}\left(\overline{z}_{\ell}\right) \\ &\quad +\sum_{u'v'}\overline{\varepsilon}_{zy,(g-u')(h-v')}e_{y,u'v'}\left(\overline{z}_{\ell}\right) \\ &\quad +\sum_{u'v'}\overline{\varepsilon}_{zz,(g-u')(h-v')}e_{z,u'v'}\left(\overline{z}_{\ell}\right)\end{aligned} \tag{62}$$

For the component $\frac{\partial h_{y,gh}(\overline{z}_\ell)}{\partial \overline{z}}$, the equation can be derived as:

$$\begin{aligned}
\partial_{\overline{y}}\sqrt{Z_0}H_z - \partial_{\overline{z}}\sqrt{Z_0}H_y &= \sum_{gh} -in_{yh}h_{z,gh}\left(\overline{z}_\ell\right)\exp\left[-i\left(n_{xg}\overline{x}+n_{yh}\overline{y}\right)\right] \\
&\quad -\sum_{m}\frac{\partial h_{y,gh}\left(\overline{z}_\ell\right)}{\partial \overline{z}}\exp\left[-i\left(n_{xg}\overline{x}+n_{yh}\overline{y}\right)\right] \\
&= i\sqrt{Y_0}\left[\overline{\varepsilon}\left(\overline{r}\right)\mathbf{E}\right]_x \\
&= i\sum_{ghuv}\overline{\varepsilon}_{xx,uv}e_{x,gh}\left(\overline{z}_\ell\right)\exp\left[-i\left(n_{x(g+u)}\overline{x}+n_{y(h+v)}\overline{y}\right)\right] \\
&\quad +i\sum_{ghuv}\overline{\varepsilon}_{xy,uv}e_{y,gh}\left(\overline{z}_\ell\right)\exp\left[-i\left(n_{x(g+u)}\overline{x}+n_{y(h+v)}\overline{y}\right)\right] \\
&\quad +i\sum_{ghuv}\overline{\varepsilon}_{xz,uv}e_{z,gh}\left(\overline{z}_\ell\right)\exp\left[-i\left(n_{x(g+u)}\overline{x}+n_{y(h+v)}\overline{y}\right)\right] \qquad (63)
\end{aligned}$$

and is simplified to be:

$$\begin{aligned}
\frac{\partial h_{y,gh}\left(\overline{z}_\ell\right)}{\partial \overline{z}} &= -in_{yh}h_{z,gh}\left(\overline{z}_\ell\right) - i\sum_{u'v'}\overline{\varepsilon}_{xx,(g-u')(h-v')}e_{x,u'v'}\left(\overline{z}_\ell\right) \\
&\quad -i\sum_{u'v'}\overline{\varepsilon}_{xy,(g-u')(h-v')}e_{y,u'v'}\left(\overline{z}_\ell\right) - i\sum_{u'v'}\overline{\varepsilon}_{xz,(g-u')(h-v')}e_{z,u'v'}\left(\overline{z}_\ell\right) \qquad (64)
\end{aligned}$$

For the component $\frac{\partial h_{x,gh}(\overline{z}_\ell)}{\partial \overline{z}}$, the equation can be derived as:

$$\begin{aligned}
\partial_{\overline{z}}\sqrt{Z_0}H_x - \partial_{\overline{x}}\sqrt{Z_0}H_z &= \sum_{gh}\frac{\partial h_{x,gh}\left(\overline{z}_\ell\right)}{\partial \overline{z}}\exp\left[-i\left(n_{xg}\overline{x}+n_{yh}\overline{y}\right)\right] \\
&\quad -\sum_{gh} -in_{xh}h_{z,gh}\left(\overline{z}_\ell\right)\exp\left[-i\left(n_{xg}\overline{x}+n_{yh}\overline{y}\right)\right] \\
&= i\sqrt{Y_0}\left[\overline{\varepsilon}\left(\overline{r}\right)\mathbf{E}\right]_y \\
&= i\sum_{ghuv}\overline{\varepsilon}_{yx,uv}e_{x,gh}\left(\overline{z}_\ell\right)\exp\left[-i\left(n_{x(g+u)}\overline{x}+n_{y(h+v)}\overline{y}\right)\right] \\
&\quad +i\sum_{ghuv}\overline{\varepsilon}_{yy,uv}e_{y,gh}\left(\overline{z}_\ell\right)\exp\left[-i\left(n_{x(g+u)}\overline{x}+n_{y(h+v)}\overline{y}\right)\right] \\
&\quad +i\sum_{ghuv}\overline{\varepsilon}_{yz,uv}e_{z,gh}\left(\overline{z}_\ell\right)\exp\left[-i\left(n_{x(g+u)}\overline{x}+n_{y(h+v)}\overline{y}\right)\right] \qquad (65)
\end{aligned}$$

and is simplified to be:

$$\begin{aligned}
\frac{\partial h_{x,gh}\left(\overline{z}_\ell\right)}{\partial \overline{z}} &= -in_{xh}h_{z,gh}\left(\overline{z}_\ell\right) + i\sum_{u'v'}\overline{\varepsilon}_{yx,(g-u')(h-v')}e_{x,u'v'}\left(\overline{z}_\ell\right) \\
&\quad +i\sum_{u'v'}\overline{\varepsilon}_{yy,(g-u')(h-v')}e_{y,u'v'}\left(\overline{z}_\ell\right) + i\sum_{u'v'}\overline{\varepsilon}_{yz,(g-u')(h-v')}e_{z,u'v'}\left(\overline{z}_\ell\right) \qquad (66)
\end{aligned}$$

To solve the fields systematically, these equations are reformulated in terms of the full fields $\mathbf{f}_{\hat{t}}$ and $\mathbf{f}_{\hat{n}}$ in the following context, and show an eigen-system problem for studied periodic structures.

A.3 Derive the coupled-wave equation of the normal field $\mathbf{f}_{\hat{n}}$

To obtain the coupled-wave equations of the normal field $\mathbf{f}_{\hat{n}}$, we consider the above-mentioned formulas for its components $h_{z,gh}(\overline{z}_\ell)$ and $e_{z,gh}(\overline{z}_\ell)$ in Equations (56) and (62), respectively, i.e.:

$$h_{z,gh}(\overline{z}_\ell) = n_{xg} e_{y,gh}(\overline{z}_\ell) - n_{yh} e_{x,gh}(\overline{z}_\ell) \tag{56}$$

$$\begin{aligned} n_{yh} h_{x,gh}(\overline{z}_\ell) - n_{xg} h_{y,gh}(\overline{z}_\ell) = & \sum_{u'v'} \overline{\varepsilon}_{zx,(g-u')(h-v')} e_{x,u'v'}(\overline{z}_\ell) \\ & + \sum_{u'v'} \overline{\varepsilon}_{zy,(g-u')(h-v')} e_{y,u'v'}(\overline{z}_\ell) \\ & + \sum_{u'v'} \overline{\varepsilon}_{zz,(g-u')(h-v')} e_{z,u'v'}(\overline{z}_\ell) \end{aligned} \tag{62}$$

Up to the Fourier order $g, h \in \{0, 1\}$, an example corresponding to Equations (56) and (62) can be matrixized:

$$\begin{bmatrix} h_{z,00}(\overline{z}_\ell) \\ h_{z,01}(\overline{z}_\ell) \\ h_{z,10}(\overline{z}_\ell) \\ h_{z,11}(\overline{z}_\ell) \end{bmatrix} = \begin{bmatrix} n_{x0} & 0 & 0 & 0 \\ 0 & n_{x0} & 0 & 0 \\ 0 & 0 & n_{x1} & 0 \\ 0 & 0 & 0 & n_{x1} \end{bmatrix} \begin{bmatrix} e_{y,00}(\overline{z}_\ell) \\ e_{y,01}(\overline{z}_\ell) \\ e_{y,10}(\overline{z}_\ell) \\ e_{y,11}(\overline{z}_\ell) \end{bmatrix} - \begin{bmatrix} n_{y0} & 0 & 0 & 0 \\ 0 & n_{y1} & 0 & 0 \\ 0 & 0 & n_{y0} & 0 \\ 0 & 0 & 0 & n_{y1} \end{bmatrix} \begin{bmatrix} e_{x,00}(\overline{z}_\ell) \\ e_{x,01}(\overline{z}_\ell) \\ e_{x,10}(\overline{z}_\ell) \\ e_{x,11}(\overline{z}_\ell) \end{bmatrix} \tag{67}$$

$$\begin{aligned} & \begin{bmatrix} \overline{\varepsilon}_{zz,00} & \overline{\varepsilon}_{zz,0-1} & \overline{\varepsilon}_{zz,-10} & \overline{\varepsilon}_{zz,-1-1} \\ \overline{\varepsilon}_{zz,01} & \overline{\varepsilon}_{zz,00} & \overline{\varepsilon}_{zz,-11} & \overline{\varepsilon}_{zz,-10} \\ \overline{\varepsilon}_{zz,10} & \overline{\varepsilon}_{zz,1-1} & \overline{\varepsilon}_{zz,00} & \overline{\varepsilon}_{zz,0-1} \\ \overline{\varepsilon}_{zz,11} & \overline{\varepsilon}_{zz,10} & \overline{\varepsilon}_{zz,01} & \overline{\varepsilon}_{zz,00} \end{bmatrix} \begin{bmatrix} e_{z,00}(\overline{z}_\ell) \\ e_{z,01}(\overline{z}_\ell) \\ e_{z,10}(\overline{z}_\ell) \\ e_{z,11}(\overline{z}_\ell) \end{bmatrix} = \begin{bmatrix} n_{y0} & 0 & 0 & 0 \\ 0 & n_{y1} & 0 & 0 \\ 0 & 0 & n_{y0} & 0 \\ 0 & 0 & 0 & n_{y1} \end{bmatrix} \begin{bmatrix} h_{x,00}(\overline{z}_\ell) \\ h_{x,01}(\overline{z}_\ell) \\ h_{x,10}(\overline{z}_\ell) \\ h_{x,11}(\overline{z}_\ell) \end{bmatrix} \\ & - \begin{bmatrix} n_{x0} & 0 & 0 & 0 \\ 0 & n_{x0} & 0 & 0 \\ 0 & 0 & n_{x1} & 0 \\ 0 & 0 & 0 & n_{x1} \end{bmatrix} \begin{bmatrix} h_{y,00}(\overline{z}_\ell) \\ h_{y,01}(\overline{z}_\ell) \\ h_{y,10}(\overline{z}_\ell) \\ h_{y,11}(\overline{z}_\ell) \end{bmatrix} - \begin{bmatrix} \overline{\varepsilon}_{zx,00} & \overline{\varepsilon}_{zx,0-1} & \overline{\varepsilon}_{zx,-10} & \overline{\varepsilon}_{zx,-1-1} \\ \overline{\varepsilon}_{zx,01} & \overline{\varepsilon}_{zx,00} & \overline{\varepsilon}_{zx,-11} & \overline{\varepsilon}_{zx,-10} \\ \overline{\varepsilon}_{zx,10} & \overline{\varepsilon}_{zx,1-1} & \overline{\varepsilon}_{zx,00} & \overline{\varepsilon}_{zx,0-1} \\ \overline{\varepsilon}_{zx,11} & \overline{\varepsilon}_{zx,10} & \overline{\varepsilon}_{zx,01} & \overline{\varepsilon}_{zx,00} \end{bmatrix} \begin{bmatrix} e_{x,00}(\overline{z}_\ell) \\ e_{x,01}(\overline{z}_\ell) \\ e_{x,10}(\overline{z}_\ell) \\ e_{x,11}(\overline{z}_\ell) \end{bmatrix} \\ & - \begin{bmatrix} \overline{\varepsilon}_{zy,00} & \overline{\varepsilon}_{zy,0-1} & \overline{\varepsilon}_{zy,-10} & \overline{\varepsilon}_{zy,-1-1} \\ \overline{\varepsilon}_{zy,01} & \overline{\varepsilon}_{zy,00} & \overline{\varepsilon}_{zy,-11} & \overline{\varepsilon}_{zy,-10} \\ \overline{\varepsilon}_{zy,10} & \overline{\varepsilon}_{zy,1-1} & \overline{\varepsilon}_{zy,00} & \overline{\varepsilon}_{zy,0-1} \\ \overline{\varepsilon}_{zy,11} & \overline{\varepsilon}_{zy,10} & \overline{\varepsilon}_{zy,01} & \overline{\varepsilon}_{zy,00} \end{bmatrix} \begin{bmatrix} e_{y,00}(\overline{z}_\ell) \\ e_{y,01}(\overline{z}_\ell) \\ e_{y,10}(\overline{z}_\ell) \\ e_{y,11}(\overline{z}_\ell) \end{bmatrix} \end{aligned} \tag{68}$$

The full-component coupled-wave equation for the normal field $\mathbf{f}_{\hat{n}}$ then can be extended as:

$$\mathbf{f}_{\hat{n}} = \begin{bmatrix} \vec{e}_z \\ \vec{h}_z \end{bmatrix} = \begin{bmatrix} -\tilde{\varepsilon}_{zz}^{-1}\tilde{\varepsilon}_{zx} & -\tilde{\varepsilon}_{zz}^{-1}\tilde{n}_x & -\tilde{\varepsilon}_{zz}^{-1}\tilde{\varepsilon}_{zy} & \tilde{\varepsilon}_{zz}^{-1}\tilde{n}_y \\ -\tilde{n}_y & 0 & \tilde{n}_x & 0 \end{bmatrix} \cdot \begin{bmatrix} \vec{e}_x \\ \vec{h}_y \\ \vec{e}_y \\ \vec{h}_x \end{bmatrix} \equiv \mathbf{D} \cdot \mathbf{f}_{\hat{t}} \tag{69}$$

Here, the symbol $\vec{(.)}$ represents a $N_g N_h \times 1$ vector, and the symbol $\tilde{(.)}$ represents a $N_g N_h \times N_g N_h$ matrix, indicating the considered $g(h)$ ranged from $g_{min}(h_{min})$ to $g_{max}(h_{max})$ with $N_g = g_{min} + g_{max} + 1 (N_h = h_{min} + h_{max} + 1)$. As indicated in Equation (69), the normal field $\mathbf{f}_{\hat{n}}$ can be obtained straightforwardly if the tangential field $\mathbf{f}_{\hat{t}}$ is given.

A.4 Derive the coupled-wave equation of the tangential field $\mathbf{f}_{\hat{t}}$

Further, we derive the coupled-wave equation of the tangential field $\mathbf{f}_{\hat{t}}$, in which the component fields of $\mathbf{f}_{\hat{n}}$ are replaced by those of $\mathbf{f}_{\hat{t}}$ via equation (69). Similarly, we consider the associated formulas of $\frac{\partial e_{y,gh}(\overline{z}_\ell)}{\partial \overline{z}}$, $\frac{\partial e_{x,gh}(\overline{z}_\ell)}{\partial \overline{z}}$, $\frac{\partial h_{y,gh}(\overline{z}_\ell)}{\partial \overline{z}}$, and $\frac{\partial h_{x,gh}(\overline{z}_\ell)}{\partial \overline{z}}$ in Equations (58), (60), (64), and (66), respectively, i.e.:

$$\frac{\partial e_{x,gh}(\overline{z}_\ell)}{\partial \overline{z}} = -in_{xg} e_{z,gh}(\overline{z}_\ell) - ih_{y,gh}(\overline{z}_\ell) \tag{60}$$

$$\frac{\partial e_{y,gh}(\overline{z}_\ell)}{\partial \overline{z}} = -in_{yh} e_{z,gh}(\overline{z}_\ell) + ih_{x,gh}(\overline{z}_\ell) \tag{58}$$

$$\begin{aligned}\frac{\partial h_{y,gh}(\overline{z}_\ell)}{\partial \overline{z}} &= -in_{yh} h_{z,gh}(\overline{z}_\ell) - i\sum_{u'v'} \overline{\varepsilon}_{xx,(g-u')(h-v')} e_{x,u'v'}(\overline{z}_\ell) \\ &\quad -i\sum_{u'v'} \overline{\varepsilon}_{xy,(g-u')(h-v')} e_{y,u'v'}(\overline{z}_\ell) - i\sum_{u'v'} \overline{\varepsilon}_{xz,(g-u')(h-v')} e_{z,u'v'}(\overline{z}_\ell)\end{aligned} \tag{64}$$

$$\begin{aligned}\frac{\partial h_{x,gh}(\overline{z}_\ell)}{\partial \overline{z}} &= -in_{xh} h_{z,gh}(\overline{z}_\ell) + i\sum_{u'v'} \overline{\varepsilon}_{yx,(g-u')(h-v')} e_{x,u'v'}(\overline{z}_\ell) \\ &\quad +i\sum_{u'v'} \overline{\varepsilon}_{yy,(g-u')(h-v')} e_{y,u'v'}(\overline{z}_\ell) + i\sum_{u'v'} \overline{\varepsilon}_{yz,(g-u')(h-v')} e_{z,u'v'}(\overline{z}_\ell)\end{aligned} \tag{66}$$

With equation (69), these equations can matrixize the coupled-wave equation of $\mathbf{f}_{\hat{t}}$ as:

$$\begin{aligned}\frac{\partial \mathbf{f}_{\hat{t}}}{\partial \overline{z}} &= i\begin{bmatrix} 0 & -1 & 0 & 0 \\ -\tilde{\varepsilon}_{xx} & 0 & -\tilde{\varepsilon}_{xy} & 0 \\ 0 & 0 & 0 & 1 \\ \tilde{\varepsilon}_{yx} & 0 & \tilde{\varepsilon}_{yy} & 0 \end{bmatrix}\begin{bmatrix} \vec{e}_x \\ \vec{h}_y \\ \vec{e}_y \\ \vec{h}_x \end{bmatrix} + i\begin{bmatrix} -\tilde{n}_x \vec{e}_z \\ -\tilde{n}_y \vec{h}_z - \tilde{\varepsilon}_{xz}\vec{e}_z \\ -\tilde{n}_y \vec{e}_z \\ -\tilde{n}_x \vec{h}_z + \tilde{\varepsilon}_{yz}\vec{e}_z \end{bmatrix} \\ &= \begin{bmatrix} \tilde{n}_x\tilde{\varepsilon}_{zz}^{-1}\tilde{\varepsilon}_{zx} & \tilde{n}_x\tilde{\varepsilon}_{zz}^{-1}\tilde{n}_x - 1 & \tilde{n}_x\tilde{\varepsilon}_{zz}^{-1}\tilde{\varepsilon}_{zy} & -\tilde{n}_x\tilde{\varepsilon}_{zz}^{-1}\tilde{n}_y \\ \tilde{\varepsilon}_{xz}\tilde{\varepsilon}_{zz}^{-1}\tilde{\varepsilon}_{zx} - \tilde{\varepsilon}_{xx} + \tilde{n}_y\tilde{n}_y & \tilde{\varepsilon}_{xz}\tilde{\varepsilon}_{zz}^{-1}\tilde{n}_x & \tilde{\varepsilon}_{xz}\tilde{\varepsilon}_{zz}^{-1}\tilde{\varepsilon}_{zy} - \tilde{\varepsilon}_{xy} - \tilde{n}_y\tilde{n}_x & -\tilde{\varepsilon}_{xz}\tilde{\varepsilon}_{zz}^{-1}\tilde{n}_y \\ \tilde{n}_y\tilde{\varepsilon}_{zz}^{-1}\tilde{\varepsilon}_{zx} & \tilde{n}_y\tilde{\varepsilon}_{zz}^{-1}\tilde{n}_x & \tilde{n}_y\tilde{\varepsilon}_{zz}^{-1}\tilde{\varepsilon}_{zy} & -\tilde{n}_y\tilde{\varepsilon}_{zz}^{-1}\tilde{n}_y + 1 \\ -\tilde{\varepsilon}_{yz}\tilde{\varepsilon}_{zz}^{-1}\tilde{\varepsilon}_{zx} + \tilde{\varepsilon}_{yx} + \tilde{n}_x\tilde{n}_y & -\tilde{\varepsilon}_{yz}\tilde{\varepsilon}_{zz}^{-1}\tilde{n}_x & -\tilde{\varepsilon}_{yz}\tilde{\varepsilon}_{zz}^{-1}\tilde{\varepsilon}_{zy} + \tilde{\varepsilon}_{yy} - \tilde{n}_x\tilde{n}_x & \tilde{\varepsilon}_{yz}\tilde{\varepsilon}_{zz}^{-1}\tilde{n}_y \end{bmatrix} \\ &\cdot i\mathbf{f}_{\hat{t}} \equiv i\mathbf{G}\cdot\mathbf{f}_{\hat{t}}\end{aligned} \tag{70}$$

Definitely, the equation (70) turns the Maxwell's curl equations into a eigen-system problems. Up to now, with the known structured layers for equations (44)-(45) and the known incidence related to equations (46)-(47), the transition behaviors of the tangential field $\mathbf{f}_{\hat{t}}$ can be formulated layer by layer via equation (70), and the corresponding normal field $\mathbf{f}_{\hat{n}}$ can be evaluated sequentially via equation (69).

In the following contexts, we continue to describe (a) the solutions of the transition fields within stack layers via equation (70), especially for these uniform layers with isotropic materials which bring in the degenerate eigen-states, and (b) the continuum of fields conditioned at interfaces between stack layers. Consequently, a complete analysis for fields through all stacks can be fulfilled, and the associated near/far field optics can be evaluated.

A.5 Eigen-system solutions

As indicated in equation (70), the tangential fields $\mathbf{f}_{\hat{t}}$ within the layers proceed an eigen-system process, in which the eigen-states are independent to each other and allow individual/straightforward analyses to evaluate the transition behaviors through the layers. At the interfaces among the layers, the tangential fields $\mathbf{f}_{\hat{t}}$ associated with the composite phases/amplitudes of the eigen-states follow the physical continuous conditions in the laboratory framework. These characteristics lead to the necessary transform between the laboratory and eigen-system frameworks as described below. Besides, for these uniform layers with isotropic materials, especially for the incident and emitted regions, the eigen-system shows the degenerate status, and a reasonable choice of the eigen-states corresponding to the physical conditions is emphasized below. Implemented with all these, the behaviors of the tangential fields $\mathbf{f}_{\hat{t}}$ through all stacks layers including the in-between interfaces can be decided. The normal fields $\mathbf{f}_{\hat{n}}$ are then obtained by equation (69), and thereby the complete light waves are understood.

A.5.1 Uniform layers with isotropic materials

For the uniform layers with isotropic materials, i.e. $\varepsilon(\overline{r})$ is a scalar constant, the coupled-wave equation of the tangential fields $\mathbf{f}_{\hat{t}}$ in equation (70) can be simplified as:

$$\begin{aligned}\frac{\partial}{\partial_{\overline{z}}}\begin{bmatrix}\vec{e}_x\\ \vec{h}_y\\ \vec{e}_y\\ \vec{h}_x\end{bmatrix} &= i\mathbf{C}\cdot\begin{bmatrix}\vec{e}_x\\ \vec{h}_y\\ \vec{e}_y\\ \vec{h}_x\end{bmatrix}\\ &= i\begin{bmatrix}0 & \tilde{n}_x\tilde{\varepsilon}^{-1}\tilde{n}_x-1 & 0 & -\tilde{n}_x\tilde{\varepsilon}^{-1}\tilde{n}_y\\ -\tilde{\varepsilon}+\tilde{n}_y\tilde{n}_y & 0 & -\tilde{n}_y\tilde{n}_x & 0\\ 0 & \tilde{n}_y\tilde{\varepsilon}^{-1}\tilde{n}_x & 0 & -\tilde{n}_y\tilde{\varepsilon}^{-1}\tilde{n}_y+1\\ \tilde{n}_x\tilde{n}_y & 0 & \tilde{\varepsilon}-\tilde{n}_x\tilde{n}_x & 0\end{bmatrix}\cdot\begin{bmatrix}\vec{e}_x\\ \vec{h}_y\\ \vec{e}_y\\ \vec{h}_x\end{bmatrix}\end{aligned} \tag{71}$$

Here, all the submatrices in $\mathbf{C}$ are diagonal and thereby the component states are independent. By straightforward calculation, its eigen-values as well as the corresponding eigen-vectors for (g,h)-order component can be obtained:

$$\begin{aligned}eigval &\equiv \kappa_{gh}\\ &= \begin{bmatrix}-\xi_{gh} & 0 & 0 & 0\\ 0 & -\xi_{gh} & 0 & 0\\ 0 & 0 & \xi_{gh} & 0\\ 0 & 0 & 0 & \xi_{gh}\end{bmatrix}\end{aligned} \tag{72}$$

with $\xi_{gh} = \sqrt{\varepsilon - n_{yh}n_{yh} - n_{xg}n_{xg}}$ while the corresponding eigen-vector matrix are:

$$eigvec = \left[\mathbf{v}'_{gh1}\ \mathbf{v}'_{gh2}\ \mathbf{v}'_{gh3}\ \mathbf{v}'_{gh4} \right] = \begin{bmatrix} \frac{-\xi_{gh}}{n_{xg}n_{yh}} & \frac{n_{xg}n_{xg}-\varepsilon_{gh}}{n_{xg}n_{yh}} & \frac{\xi_{gh}}{n_{xg}n_{yh}} & \frac{n_{xg}n_{xg}-\varepsilon_{gh}}{n_{xg}n_{yh}} \\ \frac{n_{yh}n_{yh}-\varepsilon_{gh}}{n_{xg}n_{yh}} & \frac{-\varepsilon_{gh}\xi_{gh}}{n_{xg}n_{yh}} & \frac{n_{yh}n_{yh}-\varepsilon_{gh}}{n_{xg}n_{yh}} & \frac{\varepsilon_{gh}\xi_{gh}}{n_{xg}n_{yh}} \\ 0 & 1 & 0 & 1 \\ 1 & 0 & 1 & 0 \end{bmatrix} \tag{73}$$

Due to the degeneracy in $(\kappa_{gh,1}, \kappa_{gh,2})$ and $(\kappa_{gh,3}, \kappa_{gh,4})$, the eigenvector $(\mathbf{v}'_{gh1}, \mathbf{v}'_{gh2})$ as well as $(\mathbf{v}'_{gh3}, \mathbf{v}'_{gh4})$ can be remixed by arbitrary linear combinations. Choosing

$$m_{gh} = \sqrt{n_{yh}n_{yh} + n_{xg}n_{xg}} \tag{74}$$

$$\mathbf{v}_{gh1} = \left(n_{xg}\xi_{gh}\mathbf{v}'_{gh1} - n_{xg}\mathbf{v}'_{gh2} \right) / m_{gh} \tag{75}$$

$$\mathbf{v}_{gh2} = \left(-\frac{\varepsilon_{gh}n_{yh}}{\xi_{gh}}\mathbf{v}'_{gh1} + n_{yh}\mathbf{v}'_{gh2} \right) / m_{gh} \tag{76}$$

$$\mathbf{v}_{gh3} = \left(-n_{xg}\xi_{gh}\mathbf{v}'_{gh3} - n_{xg}\mathbf{v}'_{gh4} \right) / m_{gh} \tag{77}$$

$$\mathbf{v}_{gh4} = \left(\frac{\varepsilon_{gh}n_{yh}}{\xi_{gh}}\mathbf{v}'_{gh3} + n_{yh}\mathbf{v}'_{gh4} \right) / m_{gh} \tag{78}$$

the equation (73) is then shown as:

$$eigvec = \mathbf{T}_{gh} = \left[\mathbf{v}_{gh1}\ \mathbf{v}_{gh2}\ \mathbf{v}_{gh3}\ \mathbf{v}_{gh4} \right] = \begin{bmatrix} \frac{n_{yh}}{m_{gh}} & \frac{n_{xg}}{m_{gh}} & \frac{n_{yh}}{m_{gh}} & \frac{n_{xg}}{m_{gh}} \\ \frac{n_{yh}\xi_{gh}}{m_{gh}} & \frac{\varepsilon_{gh}n_{xg}\xi_{gh}^{-1}}{m_{gh}} & \frac{-n_{yh}\xi_{gh}}{m_{gh}} & \frac{-\varepsilon_{gh}n_{xg}\xi_{gh}^{-1}}{m_{gh}} \\ \frac{-n_{xg}}{m_{gh}} & \frac{n_{yh}}{m_{gh}} & \frac{-n_{xg}}{m_{gh}} & \frac{n_{yh}}{m_{gh}} \\ \frac{n_{xg}\xi_{gh}}{m_{gh}} & \frac{-\varepsilon_{gh}n_{yh}\xi_{gh}^{-1}}{m_{gh}} & \frac{-n_{xg}\xi_{gh}}{m_{gh}} & \frac{\varepsilon_{gh}n_{yh}\xi_{gh}^{-1}}{m_{gh}} \end{bmatrix} \tag{79}$$

Hence, $\mathbf{v}_{gh1}$ and $\mathbf{v}_{gh2}$ correspond to the (g,h)-order forward TE and TM (transverse electric and transverse magnetic) representations (with respect to the plane of the diffraction wave), respectively. $\mathbf{v}_{gh3}$ and $\mathbf{v}_{gh4}$ then correspond to the backward TE and TM ones. For example, with equation (69) and (79), $\mathbf{v}_{gh1}$ denotes the component fields:

$$\mathbf{e}_{gh} = \frac{n_{yh}}{m_{gh}}\hat{\imath} - \frac{n_{xg}}{m_{gh}}\hat{\jmath} \tag{80}$$

$$\mathbf{h}_{gh} = \frac{n_{xg}\xi_{gh}}{m_{gh}}\hat{\imath} + \frac{n_{yh}\xi_{gh}}{m_{gh}}\hat{\jmath} - m_{gh}\hat{k} \tag{81}$$

along the direction $\mathbf{n_{gh}} = n_{xg}\hat{i} + n_{yh}\hat{j} + \xi_{gh}\hat{k}$. It can be seen that the characteristic fields in equations (80)-(81) associated with the eigen-solution $\propto exp(-i\xi_{gh}z)$ and constitutes the forwards TE wave. It is noted that the field amplitudes are normalized to $|\mathbf{e}_{gh}| = 1$, $|\mathbf{h}_{gh}| = \sqrt{\varepsilon}$, and $\mathbf{e}_{gh} \cdot \mathbf{n}_{gh} = \mathbf{h}_{gh} \cdot \mathbf{n}_{gh} = \mathbf{e}_{gh} \cdot \mathbf{h}_{gh} = 0$ - that is, $\mathbf{n}_{gh}$, $\mathbf{e}_{gh}$, and $\mathbf{h}_{gh}$ are mutually perpendicular. Similarly, the remaining eigen-vectors can characterize the forwards and backwards TE/TM waves and are omitted here. In this way, a unit-amplitude incident wave then can be given as $\vec{E}_q^+ = [0...1...0]^t$, $\vec{M}_q^+ = 0$ for TE wave, and $\vec{M}_q^+ = [0...1...0]^t$, $\vec{E}_q^+ = 0$ for TM wave as defined below.
Considering the full components $g_{min} \leq g \leq g_{max}$ and $h_{min} \leq h \leq h_{max}$, the coupled-wave equation (71) can be straightforwardly written as:

$$\begin{aligned} \frac{\partial}{\partial_{\overline{z}}}\mathbf{f}_{\hat{t}} &= i\mathbf{C}f_{\hat{t}} \\ \Rightarrow \frac{\partial}{\partial_{\overline{z}}}\mathbf{T}^{-1}\mathbf{f}_{\hat{t}} &= i\mathbf{T}^{-1}\mathbf{C}\mathbf{T}\mathbf{T}^{-1}f_{\hat{t}} \\ \Rightarrow \frac{\partial}{\partial_{\overline{z}}}\mathbf{q}_{\hat{t}} &= i\kappa\mathbf{q}_{\hat{t}} \quad with \quad \mathbf{f}_{\hat{t}} = \mathbf{T}\mathbf{q}_{\hat{t}} \end{aligned} \tag{82}$$

where

$$\mathbf{T} = \begin{bmatrix} \dot{\mathbf{n}}_y & \dot{\mathbf{n}}_x & \dot{\mathbf{n}}_y & \dot{\mathbf{n}}_x \\ \dot{\mathbf{n}}_y\xi & \varepsilon\dot{\mathbf{n}}_x\xi^{-1} & -\dot{\mathbf{n}}_y\xi & -\varepsilon\dot{\mathbf{n}}_x\xi^{-1} \\ -\dot{\mathbf{n}}_x & \dot{\mathbf{n}}_y & -\dot{\mathbf{n}}_x & \dot{\mathbf{n}}_y \\ \dot{\mathbf{n}}_x\xi & -\varepsilon\dot{\mathbf{n}}_y\xi^{-1} & -\dot{\mathbf{n}}_x\xi & \varepsilon\dot{\mathbf{n}}_y\xi^{-1} \end{bmatrix}, \quad \mathbf{q}_{\hat{t}} = \begin{bmatrix} \vec{E}_q^+ \\ \vec{M}_q^+ \\ \vec{E}_q^- \\ \vec{M}_q^- \end{bmatrix} \tag{83}$$

Note that $\dot{\mathbf{n}}_y$ and $\dot{\mathbf{n}}_x$ are the $N_gN_h \times N_gN_h$ diagonal matrices with diagonal elements $\frac{n_{yh}}{m_{gh}}$ and $\frac{n_{xg}}{m_{gh}}$ respectively. ξ^{-1} is the matrix with elements $1/\xi_{gh}$, not the inverse of the matrix ξ. Moreover, $\vec{E}_q^+$ and $\vec{M}_q^+$ ($\vec{E}_q^-$ and $\vec{M}_q^-$) correspond to the physical forward (backward) TE and TM waves, respectively. The transition of fields $\mathbf{q}_{\hat{t}}$ within the considered layer are now solved as:

$$\mathbf{q}_{\hat{t}}(\overline{z}) = exp\left[i\kappa\left(\overline{z} - \overline{z}_0\right)\right]\mathbf{q}_{\hat{t}}(\overline{z}_0) \tag{84}$$

A.5.2 Periodic-structured layers with isotropic/birefringent materials

For the in-between periodic layers, the transition equations of tangential fields $\mathbf{f}_{\hat{t}}$ in equation (70) can be generally expressed as:

$$\frac{\partial}{\partial_{\overline{z}}}\mathbf{q}_{\hat{t}} = i\kappa^{(a)}\mathbf{q}_{\hat{t}} \quad with \quad \mathbf{f}_{\hat{t}} = \mathbf{T}^{(a)}\mathbf{q}_{\hat{t}} \tag{85}$$

with the transition of $\mathbf{q}_{\hat{t}}$

$$\mathbf{q}_{\hat{t}}(\overline{z}) = exp\left[i\kappa^{(a)}\left(\overline{z} - \overline{z}_0\right)\right]\mathbf{q}_{\hat{t}}(\overline{z}_0) \tag{86}$$

Here, $\mathbf{T}^{(a)}$ is the eigen-vector matrix of $\mathbf{G}$ of equation (70) with column eigen-vectors, and $\kappa^{(a)}$ is the corresponding diagonal eigen-value matrix.

A.6 Boundary conditions

Now for each layer, we have been able to independently solve the transition of electromagnetic fields in the individual layers, but the continuum of fields on interfaces has still not been included. Considering the tangential components in $\mathbf{f}_{\hat{t}}$ are continuous across i_{th} interface at $\overline{z}_i$, the constriction equations can be shown as

$$\mathbf{T}_i^{(a)}\mathbf{q}_{\hat{t},i}(\overline{z}_i) = \mathbf{T}_{i+1}^{(a)}\mathbf{q}_{\hat{t},i+1}(\overline{z}_i) \tag{87}$$

Grouping this condition into the fields $\mathbf{q}_{\hat{t}}$ in equation (86), and introducing two virtual layers to consider the Fresnel refraction and reflection at surfaces of the media as described in the texts, a general expression for $N-$multilayered periodic structures can be obtained as in equation (13). This argument ignores the effects of multiple reflections as applied by (extended) Jones method, and similarly supplies as a easy-manipulated method. Further, an alternative process to consider the multiple reflections is described as below for references.
Similarly, group the equation (87) with (86), the consecutive matrix equation with undecided diffraction/reflection waves can be written as:

$$\begin{aligned}
\mathbf{q}_{\hat{t},N+1}(\overline{z}_n) &= \mathbf{T}_{N+1}^{-1}\mathbf{T}_N^{(a)}\mathbf{q}_{\hat{t},N}(\overline{z}_N) \\
&= \mathbf{T}_{N+1}^{-1}\mathbf{T}_N^{(a)}\exp\left[i\kappa_N^{(a)}\left(\overline{z}_N-\overline{z}_{N-1}\right)\right]\mathbf{q}_{\hat{t},N}(\overline{z}_{N-1}) \\
&= \mathbf{T}_{N+1}^{-1}\mathbf{T}_N^{(a)}\exp\left[i\kappa_N^{(a)}\left(\overline{z}_N-\overline{z}_{N-1}\right)\right] \\
&\quad\times(\mathbf{T}_N^{(a)})^{-1}\mathbf{T}_{N-1}^{(a)}\exp\left[i\kappa_{N-1}^{(a)}\left(\overline{z}_{N-1}-\overline{z}_{N-2}\right)\right] \\
&\quad\times\ldots \\
&\quad\times(\mathbf{T}_1^{(a)})^{-1}\mathbf{T}_0\mathbf{q}_{\hat{t},0}(\overline{z}_0)
\end{aligned} \tag{88}$$

where the first boundary is indexed as 0. Consequently, the relation between fields in the incident region 0 and in the emitted region $N+1$ can be obtained as:

$$\mathbf{q}_{\hat{t},N+1} = \begin{bmatrix} \vec{E}_{q,N+1}^{+} \\ \vec{M}_{q,N+1}^{+} \\ \vec{E}_{q,N+1}^{-} \\ \vec{M}_{q,N+1}^{-} \end{bmatrix} = \mathbf{T}_{N+1}^{-1}\mathbf{T}_N^{a}\exp\left[i\kappa_N^{a}\left(\overline{z}_N-\overline{z}_{N-1}\right)\right]\ldots(\mathbf{T}_1^{a})^{-1}\mathbf{T}_0\begin{bmatrix} \vec{E}_{q,0}^{+} \\ \vec{M}_{q,0}^{+} \\ \vec{E}_{q,0}^{-} \\ \vec{M}_{q,0}^{-} \end{bmatrix} \equiv \mathbf{W}^{-1}\begin{bmatrix} \vec{E}_{q,0}^{+} \\ \vec{M}_{q,0}^{+} \\ \vec{E}_{q,0}^{-} \\ \vec{M}_{q,0}^{-} \end{bmatrix} = \mathbf{W}^{-1}\mathbf{q}_{\hat{t},0} \tag{89}$$

or alternatively:

$$\mathbf{q}_{\hat{t},0} \equiv \begin{bmatrix} \mathbf{q}_{\hat{t},0}^{+} \\ \mathbf{q}_{\hat{t},0}^{-} \end{bmatrix} = \begin{bmatrix} \mathbf{W}_1 & \mathbf{W}_2 \\ \mathbf{W}_3 & \mathbf{W}_4 \end{bmatrix}\begin{bmatrix} \mathbf{q}_{\hat{t},N+1}^{+} \\ \mathbf{q}_{\hat{t},N+1}^{-} \end{bmatrix} = \mathbf{W}\mathbf{q}_{\hat{t},N+1} \tag{90}$$

Consider that the reflective field in the emitted region is zero, i.e. $\mathbf{q}_{\hat{t},N+1}^{-} = \begin{bmatrix} \vec{E}_{q,N+1}^{-} & \vec{M}_{q,N+1}^{-} \end{bmatrix}^T = 0$. The transmittance field in the emitted region can be obtained as:

$$\mathbf{q}_{\hat{t},N+1}^{+} = \mathbf{W}_1^{-1}\mathbf{q}_{\hat{t},0}^{+} \tag{91}$$

and the reflective field in the incident region is:

$$\mathbf{q}^{-}_{\hat{t},0} = \mathbf{W}_3\mathbf{W}_1^{-1}\mathbf{q}^{+}_{\hat{t},0} \tag{92}$$

A.7 Diffraction efficiency

To evaluate the diffraction efficiency with the obtained $\mathbf{q}^{\pm}_{\hat{t}}$, the x, y, and z components of the transmittance/reflection fields of the diffraction order (g,h) can be calculated by equations 19 (or 82, 83) and 69 for emitted/incident regions, and thereby the standard definitions of diffraction efficiency can be followed. Note that the incident fields should be excluded when calculating the reflection fields in the incident region.

B. Program codes of Wolfram Mathematica for Coupling Matrix Method

In this appendix, the program codes of Wolfram Mathematica for the (numerical) study case in the previous section are added as follows. It could be able to do the simulations by copy and paste the codes, while few characters may need to be adjusted, e.g., the superscript of W' (W'') and the power symbol on $no\hat{}2$ ($ne\hat{}2$).

```
(*Initialize one − period LC profiles (θo, φo) for single LC layer*)
dx = 0.1;  dy = dx; (*um/grid; grid interval *)
GridNx = 100; GridNy = 100;  (*grid num. in x and y *)
Λx = GridNx*dx; Λy = GridNx*dy;  (* unit cell *)
θo = Table[π*i/GridNx, {i, GridNx}, {j, GridNy}];
φo = Table[π/2.0, {i, GridNx}, {j, GridNy}];
dz = 2.0; (*um;  the thickness of the LC layer *)

(*Define optical −  related parameters*)
nI = 1.0; nE = 1.0; θ = 0.001; φ = 0.0; λ = 0.55;
ne = 1.5; no = 1.6;
grng = 1; hrng = 1;  (* − grng ≤ g ≤ grng; −hrng ≤ h ≤ hrng*)
Ng = 2*grng + 1; Nh = 2*hrng + 1; (*Note Ng < GridNx,  Nh < GridNy*)

(*Initialize relevant wave − vector matrixes related to nxg,  nyh,  respectively*)
gindx = Table[Floor[(i − 1.0)/Nh] − grng, {i, Ng*Nh}]; (* g sequence in ei or hi fields *)
hindx = Table[Mod[(i − 1), Nh] − hrng, {i, Ng*Nh}]; (* h sequence in ei or hi fields *)
nx = DiagonalMatrix[Table[nI*Sin[θ]*Cos[φ] − gindx[[i]]*λ/Λx, {i, Ng*Nh}]];
ny = DiagonalMatrix[Table[nI*Sin[θ]*Sin[φ] − hindx[[i]]*λ/Λy, {i, Ng*Nh}]];
m = DiagonalMatrix[Table[Sqrt[nx[[i, i]]^2 + ny[[i, i]]^2], {i, Ng*Nh}]];
ξ = DiagonalMatrix[Table[Sqrt[nI^2 − nx[[i, i]]^2 − ny[[i, i]]^2], {i, Ng*Nh}]];
ξinv = DiagonalMatrix[Table[1.0/Sqrt[nI^2 − nx[[i, i]]^2 − ny[[i, i]]^2], {i, Ng*Nh}]];

(*Calculate εijgh by Fourier transform of εij(x, y; z) for the single LC layer*)
εxxgh=InverseFourier[no^2+(ne^2–no^2)*Sin[θo]^2*Cos[φo]^2]/Sqrt[GridNx]/Sqrt[GridNy];
εxygh=InverseFourier[(ne^2–no^2)*Sin[θo]^2*Sin[φo]Cos[φo]]/Sqrt[GridNx]/Sqrt[GridNy];
εxzgh=InverseFourier[(ne^2–no^2)*Sin[θo]Cos[θo]Cos[φo]]/Sqrt[GridNx]/Sqrt[GridNy];
εyygh=InverseFourier[no^2+(ne^2–no^2)*Sin[θo]^2*Sin[φo]^2]/Sqrt[GridNx]/Sqrt[GridNy];
```

εyzgh=InverseFourier[(ne^2 − no^2)*Sin[θo]Cos[θo]Sin[φo]]/Sqrt[GridNx]/Sqrt[GridNy];
εzzgh=InverseFourier[no^2 + (ne^2 − no^2)*Cos[θo]^2]/Sqrt[GridNx]/Sqrt[GridNy];

(* Define the matrix εij with element εijgh *)
$\varepsilon xx = \text{Table}[0, \{i, \text{Ng*Nh}\}, \{j, \text{Ng*Nh}\}]; \varepsilon xy = \text{Table}[0, \{i, \text{Ng*Nh}\}, \{j, \text{Ng*Nh}\}];$
$\varepsilon xz = \text{Table}[0, \{i, \text{Ng*Nh}\}, \{j, \text{Ng*Nh}\}]; \varepsilon yy = \text{Table}[0, \{i, \text{Ng*Nh}\}, \{j, \text{Ng*Nh}\}];$
$\varepsilon yz = \text{Table}[0, \{i, \text{Ng*Nh}\}, \{j, \text{Ng*Nh}\}]; \varepsilon zz = \text{Table}[0, \{i, \text{Ng*Nh}\}, \{j, \text{Ng*Nh}\}];$
$\varepsilon zzinv = \text{Table}[0, \{i, \text{Ng*Nh}\}, \{j, \text{Ng*Nh}\}];$
$\text{For}[i = 1, i \leq \text{Ng*Nh}, \text{For}[j = 1, j \leq \text{Ng*Nh},$
$g = \text{gindx}[[i]] - \text{gindx}[[j]]; h = \text{hindx}[[i]] - \text{hindx}[[j]];$
$\text{gp} = \text{If}[g \geq 0, g = g + 1, g = g + \text{GridNx} + 1];$
(* follow arrangements of components in εijgh *)
$\text{hp} = \text{If}[h \geq 0, h = h + 1, h = h + \text{GridNy} + 1];$
$\varepsilon xx[[i, j]] = \varepsilon xxgh[[\text{gp}, \text{hp}]]; \varepsilon xy[[i, j]] = \varepsilon xygh[[\text{gp}, \text{hp}]]; \varepsilon xz[[i, j]] = \varepsilon xzgh[[\text{gp}, \text{hp}]];$
$\varepsilon yy[[i, j]] = \varepsilon yygh[[\text{gp}, \text{hp}]]; \varepsilon yz[[i, j]] = \varepsilon yzgh[[\text{gp}, \text{hp}]]; \varepsilon zz[[i, j]] = \varepsilon zzgh[[\text{gp}, \text{hp}]];$
$j{+}{+};]; i{+}{+};];$
$\varepsilon zzinv = \text{Inverse}[\varepsilon zz];$

(* Calculate matrix G for the single LC layer*)
$\text{G11} = \text{Dot}[\text{nx}, \varepsilon zzinv, \varepsilon xz]; \text{G12} = \text{Dot}[\text{nx}, \varepsilon zzinv, \text{nx}] - \text{IdentityMatrix}[\text{Ng*Nh}];$
$\text{G13} = \text{Dot}[\text{nx}, \varepsilon zzinv, \varepsilon yz]; \text{G14} = -\text{Dot}[\text{nx}, \varepsilon zzinv, \text{ny}];$
$\text{G21} = \text{Dot}[\varepsilon xz, \varepsilon zzinv, \varepsilon xz] - \varepsilon xx + \text{Dot}[\text{ny}, \text{ny}]; \text{G22} = \text{Dot}[\varepsilon xz, \varepsilon zzinv, \text{nx}];$
$\text{G23} = \text{Dot}[\varepsilon xz, \varepsilon zzinv, \varepsilon yz] - \varepsilon xy - \text{Dot}[\text{ny}, \text{nx}]; \text{G24} = -\text{Dot}[\varepsilon xz, \varepsilon zzinv, \text{ny}];$
$\text{G31} = \text{Dot}[\text{ny}, \varepsilon zzinv, \varepsilon xz]; \text{G32} = \text{Dot}[\text{ny}, \varepsilon zzinv, \text{nx}];$
$\text{G33} = \text{Dot}[\text{ny}, \varepsilon zzinv, \varepsilon yz]; \text{G34} = -\text{Dot}[\text{ny}, \varepsilon zzinv, \text{ny}] + \text{IdentityMatrix}[\text{Ng*Nh}];$
$\text{G41} = -\text{Dot}[\varepsilon yz, \varepsilon zzinv, \varepsilon xz] + \varepsilon xy + \text{Dot}[\text{nx}, \text{ny}]; \text{G42} = -\text{Dot}[\varepsilon yz, \varepsilon zzinv, \text{nx}];$
$\text{G43} = -\text{Dot}[\varepsilon yz, \varepsilon zzinv, \varepsilon yz] + \varepsilon yy - \text{Dot}[\text{nx}, \text{nx}]; \text{G44} = \text{Dot}[\varepsilon yz, \varepsilon zzinv, \text{ny}];$
$\text{G1i} = \text{Join}[\text{G11}, \text{G12}, \text{G13}, \text{G14}, 2]; \text{G2i} = \text{Join}[\text{G21}, \text{G22}, \text{G23}, \text{G24}, 2];$
$\text{G3i} = \text{Join}[\text{G31}, \text{G32}, \text{G33}, \text{G34}, 2]; \text{G4i} = \text{Join}[\text{G41}, \text{G42}, \text{G43}, \text{G44}, 2];$
$G = \text{Join}[\text{G1i}, \text{G2i}, \text{G3i}, \text{G4i}];$
$\text{Ta} = \text{Transpose}[\text{Eigenvectors}[G]]; (*\text{eigen} - \text{vecotr matrix}*)$
$\text{Tainv} = \text{Inverse}[\text{Ta}]; (*\text{inverse of the eigen} - \text{vecotr matrix} *)$
$\kappa\text{a} = \text{Dot}[\text{Tainv}, G, \text{Ta}]; (*\text{eigen} - \text{value matrix corresponding to the arrangement of Ta}*)$

(*Calculate the matrixes related to incidnet and emitted air regions, *i.e.* nI = nE = 1*)
$\text{nxd} = \text{DiagonalMatrix}[\text{Table}[\text{nx}[[i, i]]/m[[i, i]], \{i, \text{Ng*Nh}\}]];$
$\text{nyd} = \text{DiagonalMatrix}[\text{Table}[\text{ny}[[i, i]]/m[[i, i]], \{i, \text{Ng*Nh}\}]];$
$\text{T11} = \text{nyd}; \text{T12} = \text{nxd}; \text{T13} = \text{nyd}; \text{T14} = \text{nxd};$
$\text{T21} = \text{Dot}[\text{nyd}, \xi]; \text{T22} = \text{nI}^{\wedge}2*\text{Dot}[\text{nxd}, \xi\text{inv}]; \text{T23} = -\text{Dot}[\text{nyd}, \xi];$
$\text{T24} = -\text{nI}^{\wedge}2*\text{Dot}[\text{nxd}, \xi\text{inv}];$
$\text{T31} = -\text{nxd}; \text{T32} = \text{nyd}; \text{T33} = -\text{nxd}; \text{T34} = \text{nyd};$
$\text{T41} = \text{Dot}[\text{nxd}, \xi]; \text{T42} = -\text{nI}^{\wedge}2*\text{Dot}[\text{nyd}, \xi\text{inv}]; \text{T43} = -\text{Dot}[\text{nxd}, \xi];$
$\text{T44} = \text{nI}^{\wedge}2*\text{Dot}[\text{nyd}, \xi\text{inv}];$
$\text{T1i} = \text{Join}[\text{T11}, \text{T12}, \text{T13}, \text{T14}, 2]; \text{T2i} = \text{Join}[\text{T21}, \text{T22}, \text{T23}, \text{T24}, 2];$
$\text{T3i} = \text{Join}[\text{T31}, \text{T32}, \text{T33}, \text{T34}, 2]; \text{T4i} = \text{Join}[\text{T41}, \text{T42}, \text{T43}, \text{T44}, 2];$
$\text{Ti} = \text{Join}[\text{T1i}, \text{T2i}, \text{T3i}, \text{T4i}]; (*\text{ transform matrix Ti}*)$
$\text{Tiinv} = \text{Inverse}[\text{Ti}]; (*\text{ inverse of the transform matrix Ti} *)$

(*Solution(1) : solve diffractions and reflections with multi − reflections*)
(*set incident plane wave indfd, *e.g*. set the value of the component with$g = h = 0$ to be 1*)
indfd = Table[0, {i, 2*Ng*Nh}]; indfd[[Round[(Ng*Nh + 1)/2]]] = 1.0; (* forward incidence*)

(* Calculate the matrix Winv*)
expκ = DiagonalMatrix[Table[Exp[I*κa[[i, i]]*dz*2π/λ], {i, 4*Ng*Nh}]];
Winv = Dot[Tiinv, Ta, expκ, Tainv, Ti]; (* the total transfer matrix *)
W = Inverse[Winv];

(* Calculate the diffraction and reflection fields *)
diff1 = Table[0, {i, 2*Ng*Nh}]; ref1 = Table[0, {i, 2*Ng*Nh}]; (*initialize*)
W1 = W[[1;;2*Ng*Nh, 1;;2*Ng*Nh]];
W3 = W[[(2*Ng*Nh + 1);;4*Ng*Nh, 1;;2*Ng*Nh]];
diff1 = Dot[Inverse[W1], indfd]; (* diffraction fields *)
ref1 = Dot[W3, Inverse[W1], indfd]; (* reflection fields *)

(*Print diffraction and reflection fields as well as the corresponding g, h orders*)
Print["TE mode with multi-reflections"];
For[$i = 1, i \leq$ Ng*Nh,
Print[gindx[[i]], ", ", hindx[[i]], ", ", Abs[diff1[[i]]], ", ", Abs[ref1[[i]]]]; i++;];

(*Solution(2) : solve diffractions and reflections without multi − reflections *)
(*Calculate the matrixes related to virtual layer with $n = (\text{ne} + \text{no})/2$*)
ξavg = DiagonalMatrix[Table[Sqrt[((ne + no)/2.0)^2
− nx[[i, i]]^2 − ny[[i, i]]^2], {i, Ng*Nh}]];
ξavginv = DiagonalMatrix[Table[1.0/ξavg[[i, i]], {i, Ng*Nh}]];
T11 = nyd; T12 = nxd; T13 = nyd; T14 = nxd; T21 = Dot[nyd, ξavg];
T22 = nI^2*Dot[nxd, ξavginv]; T23 = −Dot[nyd, ξavg]; T24 = −nI^2*Dot[nxd, ξavginv];
T31 = −nxd; T32 = nyd; T33 = −nxd; T34 = nyd; T41 = Dot[nxd, ξavg];
T42 = −nI^2*Dot[nyd, ξavginv]; T43 = −Dot[nxd, ξavg]; T44 = nI^2*Dot[nyd, ξavginv];
T1i = Join[T11, T12, T13, T14, 2]; T2i = Join[T21, T22, T23, T24, 2];
T3i = Join[T31, T32, T33, T34, 2]; T4i = Join[T41, T42, T43, T44, 2];
Tavg = Join[T1i, T2i, T3i, T4i]; (* transform matrix Ti*)
Tavginv = Inverse[Tavg]; (* inverse of the transform matrix Ti *)
ClearAll[T11, T12, T13, T14, T21, T22, T23, T24, T31, T32, T33, T34, T41, T42, T43, T44];
ClearAll[T1i, T2i, T3i, T4i];

(* Calculate the transfer matrixes *)
S1 = Dot[Ta, expκ, Tainv];
Sent = Table[0, {i, 4*Ng*Nh}, {j, 4*Ng*Nh}];
Sext = Table[0, {i, 4*Ng*Nh}, {j, 4*Ng*Nh}];
W' = Inverse[Dot[Tavginv, Ti]]; W1′ = W'[[1;;2*Ng*Nh, 1;;2*Ng*Nh]];
W'' = Inverse[Dot[Tiinv, Tavg]]; W1″ = W''[[1;;2*Ng*Nh, 1;;2*Ng*Nh]];
Sent[[1;;2*Ng*Nh, 1;;2*Ng*Nh]] = Inverse[W1′]; Sent = Dot[Tavg, Sent];
Sext[[1;;2*Ng*Nh, 1;;2*Ng*Nh]] = Inverse[W1″]; Sext = Dot[Sext, Tavginv];

```
(* Calculate the diffraction and reflection fields *)
indfd2 = Table[0, {i, 4*Ng*Nh}]; indfd2[[Round[(Ng*Nh + 1)/2]]]
= 1.0; (* ignore backward *)
diff2 = Dot[Sext, S1, Sent, indfd2];

(*Print diffraction and reflection fields as well as the corresponding g, h orders*)
Print["TE mode without multi-reflections"];
For[i = 1, i ≤ Ng*Nh,
Print[gindx[[i]], ", ", hindx[[i]], ", ", Abs[diff2[[i]]]]; i++;];
```

5. References

Berreman, D. W. (1972). Optics in Stratified and Anisotropic Media: 4-by-4-Matrix Formulation, *Journal of the Optical Society of America*, Vol. 62, Iss. 4, April 1972, pp. 502-510.

Blinov, L. M.; Cipparrone, G.; Pagliusi, P.; Lazarev, V. V. & Palto, S. P. (2006). Mirrorless lasing from nematic liquid crystals in the plane waveguide geometry without refractive index or gain modulation, *Applied Physics Letters*, Vol. 89, Iss. 3, July 2006, pp. 031114-3.

Blinov, L. M.; Lazarev, V. V.; Palto, S. P.; Cipparrone, G.; Mazzulla, A. & Pagliusi, P. (2007). Electric field tuning a spectrum of nematic liquid crystal lasing with the use of a periodic shadow mask, *Journal of Nonlinear Optical Physics & Materials*, Vol. 16, Iss. 1, March 2007, pp. 75-90.

Galatola, P; Oldano, C & Kumar, P. B. S. (1994). Symmetry properties of anisotropic dielectric gratings, *Journal of the Optical Society of America A*, Vol. 11, Iss. 4, April 1994, pp. 1332-1341.

Glytsis, E. N. & Gaylord, T. K. (1987), Rigorous three-dimensional coupled-wave diffraction analysis of single and cascaded anisotropic gratings, *Journal of the Optical Society of America A*, Vol. 4, Iss. 11, November 1987, pp. 2061-2080.

Ho, I. L.; Chang, Y. C.; Huang, C. H.& Li, W. Y. (2011), A detailed derivation of rigorous coupled wave algorithms for three-dimensional periodic liquid-crystal microstructures, *Liquid Crystals*, Vol. 38, No. 2, February 2011, 241ąV252.

Jones, R. C. (1941). A new calculus for the treatment of optical systems, *Journal of the Optical Society of America*, Vol. 31, Iss. 7, July 1941, pp. 488ąV493.

Kriezisa, E. E. & Elston, S. J. (1999). A wide angle beam propagation method for the analysis of tilted nematic liquid crystal structures, *Journal of Modern Optics*, Vol. 46, Iss. 8, 1999, pp. 1201-1212.

Kriezis, E. E.; Filippov, S. K. & Elston, S. J. (2000). Light propagation in domain walls in ferroelectric liquid crystal devices by the finite-difference time-domain method, *Journal of Optics A: Pure and Applied Optics*, Vol. 2, No. 1, January 2000, pp. 27-33.

Kriezis, E. E. & Elston, S. J. (2000). Wide-angle beam propagation method for liquid-crystal device calculations, *Applied Optics*, Vol. 39, Iss. 31, November 2000, pp.5707-5714.

Kriezis, E. E.; Newton, C. J. P.; Spiller, T. P. & Elston, S. J. (2002). Three-dimensional simulations of light propagation in periodic liquid-crystal microstructures, *Applied Optics*, Vol. 41, Issue 25, September 2002 , pp. 5346-5356.

Lien, A.(1997). A detailed derivation of extended Jones matrix representation for twisted nematic liquid crystal displays, *Liquid Crystals*, Vol. 22, No. 2, February 1997, pp. 171-175.

Olivero, D & Oldano, C. (2003). Numerical methods for light propagation in large LC cells: a new approach, *Liquid Crystals*, Vol. 30, Iss. 3, 2003, pp. 345-353.

Rokushima K. & Yamakita, J. (1983). Analysis of anisotropic dielectric gratings, *Journal of the Optical Society of America*, Vol. 73, Iss. 7, July 1983, pp. 901-908.

Sutkowski M.; Grudniewski T.; Zmijan R.; Parka J. & Nowinowski K. E. (2006). Optical data storage in LC cells, *Opto-Electronics Review*, Vol. 14, No. 4, December 2006, pp. 335-337.

Witzigmann, B; Regli, P & Fichtner, W. (1998). Rigorous electromagnetic simulation of liquid crystal displays, *Journal of the Optical Society of America A*, Vol. 15, Iss. 3, March 1998, pp.753-757.

Zhang, B. & Sheng, P. (2003). Optical measurement of azimuthal anchoring strength in nematic liquid crystals, *Physical Review E*, Vol. 67, Iss. 4, April 2003, pp. 041713-9.

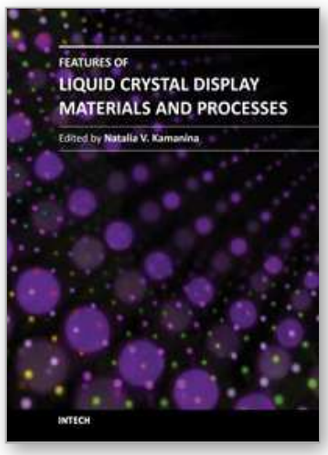

Features of Liquid Crystal Display Materials and Processes
Edited by Dr. Natalia Kamanina

ISBN 978-953-307-899-1
Hard cover, 210 pages
Publisher InTech
Published online 30, November, 2011
Published in print edition November, 2011

Following the targeted word direction of Opto- and Nanoelectronics, the field of science and technology related to the development of new display technology and organic materials based on liquid crystals ones is meeting the task of replacing volume inorganic electro-optical matrices and devices. An important way in this direction is the study of promising photorefractive materials, conducting coatings, alignment layers, as well as electric schemes that allow the control of liquid crystal mesophase with good advantage. This book includes advanced and revised contributions and covers theoretical modeling for optoelectronics and nonlinear optics, as well as includes experimental methods, new schemes, new approach and explanation which extends the display technology for laser, semiconductor device technology, medicine, biotechnology, etc. The advanced idea, approach, and information described here will be fruitful for the readers to find a sustainable solution in a fundamental study and in the industry.

InTech Europe
University Campus STeP Ri
Slavka Krautzeka 83/A
51000 Rijeka, Croatia
Phone: +385 (51) 770 447
Fax: +385 (51) 686 166
www.intechopen.com

InTech China
Unit 405, Office Block, Hotel Equatorial Shanghai
No.65, Yan An Road (West), Shanghai, 200040, China
中国上海市延安西路65号上海国际贵都大饭店办公楼405单元
Phone: +86-21-62489820
Fax: +86-21-62489821

IntechOpen